

Etude comparative de *Q. robur* et *Q. petraea*

Introduction

L'approche écophysio­logique du fonctionnement des plantes constitue sans surprise l'interface entre Ecologie et Physiologie. Ce champ de recherche permet d'appréhender les mécanismes d'adaptation aux pressions de sélection exercées par l'environnement et d'identifier le rôle des traits physiologiques impliqués dans les mécanismes de survie et de productivité des plantes au sein de leur environnement naturel. Ce type d'approche est à l'origine d'avancées majeures en termes de compréhension des mécanismes d'adaptation à des facteurs environnementaux spécifiques tels que la température, la lumière ou la disponibilité en eau. Couplés aux approches génomiques et moléculaires, les progrès apportés par l'Ecophysio­logie nous renseignent sur l'ensemble des cascades d'interactions impliquées aussi bien à l'échelle biochimique, physiologique qu'au niveau des performances globales de la plante ainsi que leurs déterminismes génétiques. Il est par ailleurs possible d'étendre l'approche écophysio­logique à un champ plus large lorsqu'il s'agit d'aborder les conséquences évolutives des traits biochimiques, physiologiques et morphologiques appliquées à l'échelle des populations ou des communautés végétales. Néanmoins, cette approche se confronte à la difficulté d'intégrer l'échelle foliaire-individuelle à l'échelle supérieure des populations et communautés, due notamment aux différentes échelles de temps impliquées. Cette étape d'intégration n'en demeure pas moins essentielle dans l'objectif de lier les mesures physiologiques de terrain aux autres domaines de recherche en écologie et biologie des populations.

Dépérissement des chênaies

Le chêne, à l'instar de toute autre espèce végétale est assujéti aux risques de son environnement. Au fil des siècles, ces aléas se sont traduits par des épisodes de dépérissement récurrents au sein des populations de chênes (Bréda et al., 2006), notamment au cours de l'Histoire récente, rapports d'archives et relevés dendrochronologiques faisant état d'évènements de stress au cours des trois dernières décennies (Thomas et al., 2008). *Quercus robur* et *Quercus petraea* n'échappèrent pas à ce phénomène. Le déclin de leurs populations respectives fut décrit au sein de nombreuses nations d'Europe, la France n'étant pas en reste (Delatour, 1983 ; Macaire, 1984 ; Thomas et al., 2002). Typiquement, ces épisodes de déclin se caractérisent par un éclaircissement généralisé du peuplement, s'étendant sur une large aire de répartition et s'accompagnant d'un faible taux de mortalité. En outre, la couronne foliaire subit une abscission anormale des rameaux associée à une mortalité des bourgeons et des

branches. A ces symptômes s'additionnent parfois décoloration des feuilles, nécrose de certains tissus et réduction de la croissance radiale de l'arbre (Hartmann and Blank, 1992). Devant l'ampleur d'un tel phénomène, la communauté scientifique et les professionnels du secteur forestier furent amenés à s'interroger sur les causes de ces dépérissements mais aussi sur la différenciation écologique des chênes sessiles et pédonculés, les deux espèces étant inégalement frappées. En effet, les premières études réalisées révélèrent une apparente fragilité de *Q. robur*, celui-ci étant plus durement touché que son homologue *Q. petraea* (Becker & Levy 1982, Durand et al., 1983, Svolba & Kleinschmit, 2000). Déterminer les origines précises du dépérissement des arbres n'est néanmoins pas chose aisée et les connaissances actuelles sur la mortalité des arbres ainsi que leurs mécanismes de tolérance aux stress environnementaux ne sont pas entièrement explicités. En Europe centrale, de nombreux facteurs aux origines biotiques et abiotiques furent associés au dépérissement des populations de chênes. En outre, Thomas et al., (2002) proposèrent un modèle conceptuel d'intégration de ces différents facteurs et parvinrent alors à la conclusion que la défoliation entomologique par les insectes ravageurs combinée à des épisodes climatiques extrêmes tels que les sécheresses estivales ou les gelées hivernales constituaient les combinaisons de facteurs susceptibles d'être à l'origine des épisodes de déclin les plus sévères. Par ailleurs, ils identifièrent que les caractéristiques hydromorphiques des sites de peuplement étaient un élément particulièrement important impliqué dans la sensibilité au stress. Ainsi, bien que lourd de conséquences, c'est à travers l'étude du dépérissement des chênaies que s'est ouverte la voie vers la caractérisation des différences écologiques entre *Q. robur* et *Q. petraea*.

Différenciation Ecologique des deux espèces

Q. petraea et *Q. robur* sont deux espèces co-occurrentes sur de nombreux sites en Europe. Elles y constituent des forêts mixtes au sein desquelles les deux espèces partagent un certain nombre de caractéristiques communes. Le chêne sessile et le chêne pédonculé sont des arbres avec une large aire de répartition colonisant une large amplitude de territoires. Cependant ils sont préférentiellement représentés sur les sols fertiles et relativement humides, conditions dans lesquelles les deux espèces deviennent dominantes au sein des systèmes forestiers (Eaton et al., 2016 ; Ellenberg, 2009). Toutefois, les chênes ne forment que rarement des forêts monospécifiques et doivent souvent faire compétition avec le Hêtre. Ainsi elles peuvent également être présentes en tant qu'espèces secondaires dans des forêts mixtes de basse altitude lorsque les sols et le climat le permettent (Ellenberg, 2009 ; Bohn et al., 2000). Les deux espèces sont capables de présenter un caractère pionnier en raison de la gamme d'environnements sur

lesquels ils sont capables de se développer. En raison de leur débourrement relativement tardif au cours de l'année, les deux espèces sont rarement exposées aux risques de gelées hivernales (Praciak et al., 2013). Les deux espèces développent des systèmes racinaires profonds leur conférant un ancrage solide et leur permettant de prospector le sol efficacement (Praciak et al., 2013 ; Savill, 2013). Malgré les nombreux traits communs aux deux espèces, leurs niches écologiques de prédilection divergent considérablement l'une de l'autre. Ainsi *Q. robur* affiche une tendance à grandir sur des sols chargés sous un climat plus continental ainsi que des régions humides le long des cours d'eau parfois sujettes aux inondations. En revanche, *Q. petraea* est considéré comme étant plus tolérant au stress hydrique, il se développe aisément sous un climat atlantique et des sols drainés et acides moins chargés en nutriments et parfois particulièrement rocheux. Il n'est pas rare de le répertorier le long des pentes ou au sommet de petits reliefs (Praciak et al., 2013 ; Jones, 1959; Savill, 2013 ; Aas et al., 2000 ; Aas et al., 2012). Les deux espèces sont exigeantes en terme d'accès à la lumière, plus particulièrement *Q. robur* (Praciak et al., 2013 ; Savill, 2013). De manière générale il est donc admis que *Q. robur* et *Q. petraea* présentent des niches écologiques clairement différenciées notamment par rapport à l'accès à l'eau et à leurs tolérances respectives pour le stress hydrique.

Bien qu'il soit communément admis au sein de la littérature que *Q. petraea* soit disposé à une meilleure tolérance à la sécheresse que *Q. robur*, nécessité est de mentionner l'existence d'une large gamme de tolérance à ce stress au sein du genre *Quercus* (Table 1 : d'après Dickson & Tomlinson, 1996). Aussi convient-il de relativiser l'étude comparative réalisée dans le cadre de ces travaux de thèse à l'échelle du genre *Quercus*.

Species name	Common name	Water Stress
<i>Q. rubra</i>	Northern red oak	Sensitive
<i>Q. shumardii</i>	Shumard oak	Sensitive
<i>Q. robur</i>	Pedunculate oak	Sensitive
<i>Q. petraea</i>	Sessile oak	Intermediate
<i>Q. velutina</i>	Black oak	Intermediate
<i>Q. coccinea</i>	Scarlet oak	Intermediate
<i>Q. macrocarpa</i>	Bur oak	Intermediate
<i>Q. muehlenbergii</i>	Chinkapin oak	Intermediate
<i>Q. marilandica</i>	Blackjack oak	Tolerant
<i>Q. stellata</i>	Post oak	Tolerant
<i>Q. laevis</i>	Turkey oak	Tolerant
<i>Q. gambelii</i>	Gambel oak	Tolerant

Table 1 : Classification relative de la tolérance à un stress hydrique de quelques espèces du genre *Quercus*. (D'après Dickson & Tomlinson 1996)

Afin d'éviter de trop nombreuses récurrences entre articles et corps de texte de ce manuscrit, l'état de l'art traitant les différences écophysiologiques sur les plans anatomiques et physiologiques entre les espèces est intégré au dernier chapitre de synthèse de ces travaux.

Le projet H2Oak (2014-en cours) : (*Q.petraea*, *Q.robur*)

Dans un contexte de changements climatiques, l'optimisation de la production de biomasse et la limitation de la consommation en eau par les plantes revêtent une importance toute particulière en gestion forestière. Focalisé sur la diversité des traits adaptatifs liée à l'efficacité d'utilisation de l'eau (WUE), le projet ANR H2Oak a été initié en 2014 sous l'égide du Docteur Oliver Brendel (coordinateur de ces travaux). Les objectifs de ce projet sont de déterminer dans quelle mesure WUE et les traits sous-jacents de l'efficacité jouent un rôle en termes d'incidence sur le fitness, d'adaptation de différentes provenances de chênes en fonction de leurs provenances et donc leurs conditions environnementales d'origine et s'il existe une diversité génétique suffisante au sein des populations pour répondre à la demande adaptative future liée aux changements climatiques. En outre, H2Oak combine des approches d'écologie des populations et d'écophysiologie de la plasticité de réponse à la sécheresse soutenues par les apports de la génétique des populations. Ce travail de thèse s'inscrit au sein du volet écophysiologique du projet H2Oak. De manière générale, H2Oak aspire à identifier chez le chêne les régions du génome associées à l'efficacité d'utilisation de l'eau (WUE), de caractériser la diversité de plasticité de réponse à la sécheresse ainsi que d'établir une liste de gènes candidats à l'aide de populations acclimatées à un gradient de stress hydrique, afin d'étudier l'adaptation de leurs régénérations naturelles au sein d'un système de sylviculture.

Objectifs

Ce deuxième chapitre avait pour objectif de déterminer les causes physiologique et/ou anatomiques de la variabilité de l'efficacité d'utilisation de l'eau (WUE) à travers plusieurs échelles d'intégration de l'efficacité, allant de mesures instantanées d'échanges gazeux foliaires en conditions naturelles ou contrôlées (W_i) à des mesures intégrées dans le temps de la composition isotopique foliaire ($\delta^{13}C$) et l'efficacité de transpiration (TE). Nous nous sommes par la suite attachés à décrire les éventuelles différences observables entre les deux espèces de chênes aussi bien en conditions non limitantes qu'en conditions de stress hydrique, explorant ainsi la plasticité de réponse à la sécheresse de WUE et de ses traits sous-jacents chez *Q. robur* et *Q. petraea*.

Afin de répondre à ces objectifs, deux expérimentations ont été réalisées en 2015 et en 2017.

Au cours de la première année de thèse (2015) nous avons réalisé une première étude comparative entre *Q. robur* et *Q. petraea*. A cette fin, nous avons planté en serre des glands provenant de deux forêts monospécifiques originaires de la même région forestière (Vallée de la Soane). La moitié des jeunes chênes devant par la suite être assujettie à une forte sécheresse expérimentale, nous avons préalablement constitué des sous-groupes au sein de chaque espèce sur les bases d'un screening phénotypique de l'efficacité d'utilisation de l'eau intrinsèque (Wi). Cette sélection initiale assurant une gamme d'efficacité comprenant des phénotypes extrêmes ainsi qu'une distribution gaussienne des phénotypes d'efficacité au sein de chaque sous-groupe. Suite à cette sélection, la moitié des plantes fut soumise à des conditions hydriques limitantes. Un ensemble de campagnes de mesures explorant les échanges gazeux foliaires ainsi que la dynamique de réponse stomatique à la lumière fut alors réalisée. Les plantes furent enfin récoltées et tout un ensemble de variables biologiques mesuré (détaillé dans la première publication de ce chapitre : Article 2). Il faut par ailleurs noter que pendant l'ensemble de cette expérimentation la consommation hydrique individuelle des plantes fut comptabilisée grâce à un dispositif automatique d'arrosage et de pesée permettant à l'issue de la récolte d'estimer l'efficacité de transpiration des chênes (TE). Cette expérimentation fut également l'occasion de co-encadrer un stage pédagogique d'initiation à la recherche (Clark Raveloson - Master 1), dans la continuité de la mission de doctorant contractuel chargé d'enseignement exercée en parallèle de ces travaux de thèse (deux années).

Lors de la seconde étude comparative (2017), nous avons étudié 2 provenances de *Q. petraea* et 2 populations de *Q. robur* sélectionnées en fonction d'un gradient de stress hydrique des sites de provenance afin d'élargir la variabilité intra-spécifique de chaque espèce. Une approche différente de mise en place du stress fut choisie, l'ensemble des jeunes arbres ont ainsi été progressivement soumis à des conditions de stress hydrique de plus en plus intenses (détaillées dans la deuxième publication de ce chapitre : Article 3). Ce faisant, nous avons pu explorer la plasticité de réponse des échanges gazeux foliaires de ces deux espèces à une sécheresse progressive. En parallèle de ce suivi nous avons monitoré la dynamique de croissance radiale et verticale des jeunes plants. Additionnellement, deux campagnes de mesures d'échanges gazeux foliaires sur les mêmes pousses furent menées à deux stades spécifiques de la mise en sécheresse, espacées d'un mois l'une de l'autre : l'une en début d'expérimentation sous conditions non limitantes, l'autre à un stade de sécheresse modérée, nous permettant d'explorer à travers d'autres mesures la plasticité de réponse des échanges gazeux foliaires mais aussi de la capacité photosynthétique ainsi que la dynamique de réponse stomatique à la lumière des

deux espèces de chênes. Cette seconde étude comparative offrit également la possibilité de rédiger ainsi que co-encadrer un stage de recherche (Jimmy Wyss - Master 2).

L'approche par modélisation de la dynamique des échanges gazeux foliaires constitue une part importante de ces travaux de thèse. Cette approche fut en effet employée au cours de l'ensemble des quatre expérimentations réalisées entre 2015 et 2017. Une synthèse de ces travaux est par ailleurs dressée dans le dernier chapitre de ce manuscrit. Les campagnes de mesures de dynamique réalisées en 2015 (publication 2) constituèrent les travaux préliminaires de cette approche, nous permettant d'explorer chez les deux espèces la vitesse de réponse stomatique ainsi que sa plasticité de réponse à la sécheresse. A l'instar de WUE, nous avons visé à déterminer les traits physiologiques et/ou anatomiques liés à la dynamique de réponse stomatique à la lumière ainsi que WUE elle-même à travers ses différentes échelles d'intégration. Nous avons décidé de poursuivre les travaux exploratoires de 2015 en réitérant des campagnes de mesures de la dynamique stomatique au cours de l'expérimentation de 2017 (publication 3) et complétant les autres travaux réalisés sur le sujet (publication 1 : chapitre II (tabac) et publication 4 chapitre IV (*Q. petraea* uniquement)). Ces campagnes avaient également pour objectifs d'explorer la plasticité de la dynamique sous sécheresse. Néanmoins, il fut décidé de modifier légèrement le protocole de mesures (intensité des changements de lumière ainsi que leur nombre) afin d'explorer dans une plus large mesure la dynamique de réponse des stomates à la lumière.

Les résultats de ces deux études comparatives sont présentés au sein de ce chapitre sous forme de deux publications relatives spécifiquement à chacune des expérimentations. Ces deux publications sont synthétisées et mises en perspective dans le dernier chapitre de ce manuscrit.

Article 2 : Etude comparative de Q. robur et Q. petraea (H2Oak 2015)

Biomass accumulation drives whole plant transpiration efficiency differences between two related sympatric oaks species: importance of underground biomass production in response to drought in Quercus robur & Quercus petraea seedlings

Théo P. H. Gérardin¹, Didier Le Thiec and Oliver Brendel^{1,2}

Adresses:

¹Université de Lorraine, AgroParisTech, INRA, Silva, F-54000 Nancy, France

²Corresponding author postal address: Oliver Brendel, INRA, UMR Silva, F-54280 CHAMPENOUX, France

Tel : 00 33 383394100

ORCID :

Théo P.H. Gérardin: <https://orcid.org/0000-0002-5427-6470>

Didier Le Thiec: <https://orcid.org/0000-0002-4204-551X>

Oliver Brendel: <https://orcid.org/0000-0003-3252-0273>

Emails: tgerardin.phd@gmail.com, didier.lethiec@inra.fr, oliver.brendel@inra.fr

Keywords: drought, dynamic response, root system, transpiration efficiency, growth, oak

Highlights

- Oaks species display faster stomatal dynamics to light under water stressed conditions
- Different irradiance closing steps induce similar dynamic responses regardless of the stomatal amplitude
- Q. petraea and Q. robur seedlings display similar growth and gas exchanges rates under progressive drought

Abstract

While most of comparative studies between the two sympatric and closely related oak species (*Q. robur* and *Q. petraea*) established differences in water use efficiency, not much is known about the underlying traits driving these differences. We assessed water use efficiency at different temporal levels from leaves instantaneous gas measurements to whole plants transpiration efficiency and measured numerous physiological and morphological traits on *Q. petraea* and *Q. robur* seedlings grown under control and drought conditions. Our objectives were to determine the plasticity of water use efficiency to drought and to which physiological as well as morphological factors these differences were related. We found no species difference for intrinsic water use efficiency, however, *Q. robur* seedlings displayed significantly higher transpiration efficiency than *Q. petraea* in both treatments. These differences were mainly driven by differences in biomass accumulation rather than water use, especially due to variation in the root biomass. Both species also differed in their carbon allocation strategy as a probable acclimation to water stress, *Q. petraea* invested relatively more in its root systems than *Q. robur* although globally producing less biomass. At the leaf level, drought increased the speed of stomatal dynamics to irradiance changes, whereas no response of stomatal morphology was detected. Although faster dynamics under water stressed conditions were in accordance with previously hypothesized contribution of stomatal dynamics to whole plant water use, no clear links were established for oaks seedlings.

Table 1 : List of abbreviation

var	unit	Variable explanation	n obs
LS	cm ²	Total plant Leaf surface	59
FRS	cm ²	Fine roots surface	FRS=FRBm/RMA*1000 22
RSSr	-	Rootshoot surface ratio	FRS/LS 22
LBm	g	Leaf biomass	62
LMA	g /cm ²	Leaf mass area	FBm/ LS 59
LRWC	%	Leaf relative water content	32
Osm	mmol/ kg	Leaf osmolarity	32
SBm	g	Stem biomass	62
BBm	g	Branch biomass	60
Bn	-	Branch number	62
RMA	mg /cm ²	Fine root masse per area	22
CRBm	g	Coarse root biomass	23
FRBm	g	Fine root biomass	23
CFRBm	g	Fine and Coarse Root biomass	CRBm+FRBm 62
CRBmr	%	Coarse root proportion	CRBm / RBm 23
FRBmr	%	Fine root proportion	FRBm / RBm 23
Rr	-	Coarse/fine roots ratio	CRBm/FRBm 23
TRn	-	Tap root number	62
TRBm	g	Tap root biomass	62
TRBmr	%	Overall tap root proportion	TRBm / UGBm 62
RBm	g	Root biomass	TRBm+CRBm+FRBm 62
WBm	g	Woody biomass	BBm + SBm 62
AGBm	g	Above ground biomass	BBm + SBm + LBm 62
TBm	g	Total biomass	AGBm+RBm 62
RS	-	Root-shoot ratio	RBm / AGBm 62
FS	-	Foliar-shoot ratio	LBm / AGBm 62
BSr	-	Branch over stem biomass ratio	BBm/SBm 62
H	cm	Plants final height	62
D	mm	Plants final diameter	62
OL	μm	Ostiole length	32
GCL	μm	Guard cells length	32
GCW	μm	Guard cells width	32
SC	-	Stomatal pore coefficient	OL/GCL 32
SS	μm ²	Stomatal size	$\pi*(GCL/2)*(GCW/2)$ 32
SD	stomata / mm ²	Stomatal density	32
TWCS	L/cm ²	Total Water Consumption standardized by plant surface	TWC/LS 59
BmS	g/cm ²	Biomass produced standardized by plant surface	Bm/LS 54
TWC	L	Total Water Consumption during the TE monitoring period	62
Bm	g	Biomass produced during the TE monitoring period	TBm - iB 57
iBm	g	Initial biomass	62
TE	g.L ⁻¹	Transpiration efficiency	Bm/H2O 57
δ ¹³ C		¹³ C isotopic composition in leaves	30
N	%	Nitrogen concentration in leaves	30
C	%	Carbon concentration in leaves	30
Vmax	μmol CO ₂ m ⁻² s ⁻¹	Maximum RubisCo activity	27
Jmax	μmol e ⁻ m ⁻² s ⁻¹	Maximum potential electron transport rate	27
A _n aci	μmol CO ₂ m ⁻² s ⁻¹	Carbon assimilation from Aci curves at 400ppm CO ₂	27
g _s aci	mol H ₂ O m ⁻² s ⁻¹	Stomatal conductance from Aci curves at 400ppm CO ₂	27
	μmol CO ₂ mol ⁻¹		
Wi aci	H ₂ O	Intrinsic water use efficiency from Aci curves at 400ppm CO ₂	A aci / g aci 27
A _n PPFD	μmol m ⁻² s ⁻¹	Net CO ₂ assimilation from response curves at SS1	26
g _s PPFD	mol m ⁻² s ⁻¹	Stomatal conductance from response curves at SS1	26
wi	μmol CO ₂ mol ⁻¹		
PPFD	H ₂ O	Intrinsic water use efficiency from response curves	An- PPFD / g _s - PPFD 26
Ci PPFD	μmol mol ⁻¹	Internal CO ₂ concentration from light curves	26
λ cl	sec	Closing lag time	25
τ cl	sec	Closing response time	25
SL cl	mol m ⁻² s ⁻²	Closing maximal slope	25
λ op	sec	Opening lag time	22
τ op	sec	Opening response time	22
SL op	mol m ⁻² s ⁻²	Opening maximal slope	22
τ r	-	Tau closing/opening ratio	τ cl / τ op 22
λ r	-	Lambda closing/opening ratio	λ cl / λ op 22

SLr	-	Slope closing/opening ratio	SL cl / SL op	22
SA	$\text{mol m}^{-2} \text{s}^{-1}$	Stomatal amplitude of variation during light curves		25
RSA	%	Relative stomatal amplitude of variation during light curves		25
Gstart	$\text{mol m}^{-2} \text{s}^{-1}$	Stomatal conductance at steady state SS1		25
gend	$\text{mol m}^{-2} \text{s}^{-1}$	Stomatal conductance at steady state SS2/SS3		25
NT	mg.min^{-1}	Nocturnal transpiration		62
DT	mg.min^{-1}	Daily transpiration (including day and night)		62
NTS	$\text{mg.min}^{-1}/\text{cm}^2$	Nocturnal transpiration per leaf surface	NT/SF	59
DTS	$\text{mg.min}^{-1}/\text{cm}^2$	Daily transpiration per leaf surface	DT/SF	59
NDR	%	Nocturnal transpiration proportion over the day	(NT/DT)*100	62

Introduction

The two most common oak species in western Europe, *Quercus robur* and *Quercus petraea* are two sympatric broad-leaf forest tree species displaying different ecological behaviours despite a high genetic proximity (Bacilieri et al. 1995, Scotti-Saintagne et al. 2004). *Q. robur* is frequent on soils with high nutrient and water availability (Lévy et al. 1992) whereas *Q. petraea* is more likely to be found on well drained soils. However, *Q. robur* is able to colonize habitats not matching its actual ecological niche which led to *Q. robur* occurrences on soils with poor nutrient availability or short water storage as a result of management practices and because both species display pioneering ecological characteristics (Becker and Lévy, 1982).

Oaks are affected by recurrent and important decline episodes whose main cause has been identified as drought (Landmann et al. 1993), however, the symptoms and several other causal factors involved in such declines vary in many european countries (Thomas et al. 2002). Despite their sympatric repartition, it has often been reported that *Q. robur* was subjected to severe declines after drought events while *Q. petraea* was much less affected (Bréda et al. 1993). The reasons of such different ecological requirements have not been clearly assessed.

Various studies have investigated the possible ecophysiological traits involved in the differences in drought tolerance between the two-oak species. *Q. robur* has often been described as more vulnerable to water-stress due to higher reductions of stomatal conductance as well as water potential induced by drought compared to *Q. petraea* (Cochard et al. 1992, Tyree and Cochard 1996, Gieger et al. 2002). Both species were recorded with different levels of hydraulic conductivities in roots and shoots, ultimately leading to differences in cavitation resistance (Nardini et al. 1999), but also displayed contradictory results in other publications with similar root hydraulic conductivity and pressure (Rasheed-Depardieu et al. 2012). Moreover, similar responses to drought of the two species were described, such as similar afternoon water potentials (Gieger et al. 2005) and same turgor loss thresholds and osmotic pressures at maximum turgor (Thomas et al. 2000).

Differences in biomass allocation between the two species have also been observed. From the numerous studies on growth and biomass production figuring both species, *Q. robur* seedlings have

almost always been described as producing more biomass and growing faster than *Q. petraea* under well irrigated, as well as drought stress conditions (Ponton et al. 2001, Kuster et al. 2013). However, similar growth rates and thresholds of growth drought response have also been reported for both species (Sanders et al. 2014). For belowground traits, lower root dry mass to root surface area ratios in *Q. petraea* (Nardini et al 1999) or shallower root systems in *Q. robur* (Bréda et al. 1993) have been observed. In both oak species, an increased production of fine-roots has also been identified as an acclimation to drought (*Q. robur*: Osonobi & Davies 1981, Van hees 1997; *Q. petraea* : Thomas 2000), However, Gieger et al. (2002) suggested that both species acclimated differently to drought, *Q. petraea* by reducing its leaf mass and *Q. robur* by maintaining the leaf mass but slightly increasing the fine roots biomass.

Regarding leaf morphology, higher values of total leaf biomass and area have been reported in *Q. robur* (Günthardt-Goerg et al. 2013) However, contrasting results have been published for leaf mass per area (LMA), i.e. both species have been described with similar LMA values (Thomas et al. 2000, Günthardt-Goerg et al. 2013) while higher LMA in *Q. robur* seedlings were described in another study (Steinbrecher et al. 2013). Moreover, the leaf morphology of both species is known to change with trees aging (Kleinschmit et al. 1995), contributing to the difficulty to draw a firm conclusion on their interspecific differences. Only a few studies reported differences associated to different ecological behaviours between the two species such as lower leaf area and biomass in *Q. petraea* compared to *Q. robur* in response to drought (Gieger et al. 2005). Overall it seems that differences between the two species depend much on the experimental set-up. Furthermore, there is a lack of information about the differences between the two-oak species under control conditions and soil water deficit for the traits related to the stomatal anatomy and behaviour as well as estimations of whole plant water use efficiency.

At any time, plants are functioning by compromising between the uptake of CO₂ for carbon assimilation and water vapour loss through gas exchange via the stomata. This compromise is often referred as water use efficiency (WUE) and can be studied at several levels. At the leaf level, WUE is an instantaneous and direct calculation of the ratio between the net CO₂ assimilation (A_n) and the stomatal conductance for water vapour (g_s) named intrinsic water use efficiency (W_i , $\mu\text{mol CO}_2 \text{ mol}^{-1} \text{ H}_2\text{O}$). Farquhar and Richards (1984) established a negative relationship between W_i and the bulk leaf isotopic decomposition for ¹³C ($\delta^{13}\text{C}$) allowing a practical proxy estimation of W_i on large sample sizes. $\delta^{13}\text{C}$ in wood material integrates (non-linearly) over time and across the trees crown but remains a reliable estimate of leaf level W_i . At the whole plant level and over time, WUE can be integrated as the ratio between the overall dry biomass produced by the plant and its total water consumption over the same period and is referred as transpiration efficiency (TE, $\text{g L}^{-1} \text{ H}_2\text{O}$). The calculation of TE requires a

precise monitoring of the water consumed as well as the final, destructive harvesting of the plants. Due to these experimental constraints, estimations of TE in tree species are rare in the literature (Guehl et al. 1993, Cernuzak et al. 2007, Roussel et al. 2009). Numerous studies focused on water use efficiency through its different estimators either in *Q. robur* (i.e. Picon et al. 1996, Welander et al. 2000, Roussel et al 2009) or in *Q. petraea* (Guehl et al. 1995, Chevillat et al. 2005). However, fewer studies investigated both species (i.e Wagner et al. 1997, Steinbrecher et al. 2013, Rasheed-Depardieu et al. 2015) and only a few of them were comparative studies assessing the differences between the two-oak species (Thomas et al. 2000, Ponton et al. 2002, Pflug et al. 2015). Interspecific differences have been reported, *Q. petraea* displaying generally a higher water use efficiency than *Q. robur* (Epron and Dreyer 1993; Ponton et al. 2001) but this is not always consistent in literature since both species sometimes display similar values (Thomas et al. 2000, Hu et al. 2013) or even possible opposite observations (Thomas et al. 2008 : not tested statistically). However, the small number of comparative studies and the fact that highly different experimental designs prevent to draw any firm conclusion about the inter-specific differences based on the current literature. Furthermore, WUE in oak has also been associated with a large intraspecific variability (Brendel et al. 2008) and plasticity under drought (Ponton et al 2002). At the leaf level, stomatal conductance (g_s) has been reported as the main driver of W_i under both control (Roussel et al. 2009a; *Q. robur*) and drought conditions (Ponton et al. 2002; both species) underlying the important role of the stomatal regulation on gas exchange. However, to our knowledge, no comparative study has been conducted on *Q. robur* and *Q. petraea* using an experimental drought to explore differences in stomatal regulation and their impact on the different levels of WUE as well as other underlying physiological and morphological traits.

Leaf level WUE depends largely on stomatal regulation, which in turn depends on morphology as well as physiology. Morphological traits such as stomatal density and size have been found to set the maximal aperture of the stomata and therefore the maximal stomatal conductance (Franks & Farquhar 2001, Dow et al. 2014). Variations in stomatal morphology have been linked to variations in instantaneous and long-term WUE through g_s (Doheny-Adams et al 2012, Franks et al. 2015), suggesting that stomatal morphology might be an interesting target for manipulation to improve WUE (Violet-chabrand et al. 2017). Moreover, in a *Q. robur* full-sib family Roussel et al. (2008) established a relationship between the expression of ERECTA, a gene known to modulate stomatal density and WUE (Masle et al. 2005) as their results shown a co-variation between W_i , g_s and ERECTA expression.

Leaves are submitted to a rapidly fluctuating atmospheric environment with strong variations of light, vapor pressure deficit between the leaf and the atmosphere (VPD), temperature and/or soil water deficit and therefore a need to balance gas exchange by adjusting the stomatal conductance continuously during the diurnal cycle (Percy et al. 2000). Compared to stomatal dynamics in response

to changes of irradiance, the variation of net CO₂ assimilation, if not limited by g_s , varies much faster, usually a few seconds. Therefore, a short-term fluctuation of environmental conditions can lead to a temporal decoupling between A_n and g_s (Lawson et al. 2010; McAusland et al. 2016, Vialet-Chabrand et al. 2017). Such non-synchronicity in temporal responses of gas exchanges may have major repercussions on the carbon fixation through photosynthesis, the water lost by transpiration and thus the water use efficiency (Lawson et al. 2010). Vico et al. (2011) linked plant functional types and water availability to stomatal responses, where plants from dryer climates displayed faster stomatal responses. Ooba and Takahashi (2003) observed among numerous species an asymmetric stomatal response between closing and opening and suggested that the symmetry might be related to the growing conditions and provide ecological advantages during dynamic gas exchanges such as improved assimilation associated to a faster opening under light limited environments. Furthermore, Roussel et al. (2008) put in evidence highly divergent daily time-courses of stomatal conductance between extreme WUE genotypes of oaks seedlings. Altogether, these results tend to suggest a link between WUE and the dynamic response to environmental changes.

Studies have investigated the dynamics of stomatal response and photosynthesis to fluctuating light (Kirschbaum et al. 1988; Lawson et al. 2010; McAusland et al. 2016; Kardiman and Raebild, 2018; Matthews et al. 2018). Over time, these fluctuations drive the temporal dynamics of carbon gain, water loss and by extension plants water use efficiency (Lawson and Blatt, 2014).

While numerous studies on water use efficiency characterization among the two oaks species have been published, the physiological and morphological traits underlying WUE variations were not assessed systematically and there is therefore a lack of knowledge of the origin of the differences in TE observed. We explored TE and underlying traits at different levels of integration. Our main objectives were to:

(i) characterize the impact of drought on TE and underlying traits, (ii) assess the differences between two oak species for TE and underlying traits as well as their plasticity to drought and (iii) identify which morphological and physiological traits drive the variability in TE independently of species and treatment.

Material and methods

Plant material and experimental design

The experiment was carried out on *Q. robur* and *Q. petraea* at the National Institut of Agronomical Research (INRA), Champenoux, France (48°45'8"N, 6°20'28"E, 259m). The acorns used were collected in 2015 from mature trees of *Q. robur* and *Q. petraea* in natural oaks pure stands in the « Vallée de la Saône », France, respectively in the Communal forest of Perrigny-sur-l'Ognon and the Domanial forest of Longchamp. The sites were characterised by similar atmospheric (or climatic) conditions. Collected acorns from both species were weighed and then sown in 6L pots filled with a 5/3/2 (V/V/V) mixture of sand, peat and silty-argillaceous forest soil, respectively. The seedlings stayed during the early spring 2015 in a nursing greenhouse for two weeks and then were transferred in a greenhouse equipped with a robotic system allowing automatized plants (Bogeat et al. 2019, Durand et al. 2019) weighting and watering in which they stayed during the whole experiment (for six months from sowing on March 3rd to the final harvest on September 2nd). Each pot was watered to reach an individual target-weight aiming to a given soil water content. 64 of the 72 available positions of the robotic system were used for the plants included in the experiment, 4 additional positions were occupied by 4 nonplanted empty pots (two for each water treatment) dedicated to the calculation of soil water evaporation, used in the correction of plants total water consumption. The two species were positioned alternatively in the six rows of the robotic system and submitted to the same growing conditions: natural growth light and well irrigated conditions (irrigated daily) until drought establishment, while being well fertilized during the whole experiment (two treatments of 15g Nutricot T100, 13:13:13 NPK and micronutrients; Fertil SAS, Boulogne-Billancourt, France). Initially two acorns were sown in each pot to ensure a successful establishment and an intra-specific diversity, resulting in 64 acorns per species. After a first screening of W_i (described below), one of the two plants in a pot was harvested, to maximize diversity in W_i by keeping intentionally the WUE extremes within each species. The remaining 32 plants of each species were allocated to drought and control groups, maintaining a maximum diversity of W_i for each group.

Measurement of soil water status and drought establishment

The volumetric soil water content was measured by time domain reflection (TRIME-TDR; IMKO GmbH, Ettlingen, DE) in each pot at about 10cm depth on a regular basis of 1 measurement per week throughout the experiment. Air temperature inside the greenhouse followed the environmental variations but never exceeded 25°C due to a cooling system in the study facility. All the plants were allowed to grow under well irrigated and fertilized conditions for 4 months (soil water content above 25%). Then in early July the weighting target of every plants were lowered in order to reach 23%

volumetric soil water content (SWC; 85% of relative extractable water content: REW_{soil}) and 9% SWC (17% of REW_{soil}) of volumetric soil water content under control and drought treatments until the end of the experiment 2 month later.

$$REW_{soil} = ((SWC - SWC_{wilt\ point}) / (SWC_{field\ capacity} - SWC_{wilt\ point})) * 100$$

With SWC at wilting point =3%: SWC at field capacity =33%

Gas exchanges measurements

The initial screening of W_i was conducted with a gas exchange system (Li-Cor 6200; LI-COR, Lincoln, NE, USA). Leaves from the first and second flushes were selected. Net CO₂ assimilation rate (A) and stomatal conductance for water vapour (g_s) were measured then W_i was calculated as the ratio between A and g_s . 7 measures (4 on one first flush leaf and 3 one second flush leaf per plant) were made in order to characterize the water use efficiency variability among species. Based on these measurements, we established one population following a normal distribution for W_i in each species, later divided among treatments (see annexe 2 for further information).

Stomatal kinetics under light change

Gas exchanges were measured using a portable photosynthesis system (Li-Cor 6400; LI-COR, Lincoln, NE, USA) equipped with a 2 cm² leaf chamber. All measurements were carried out between 07:00 and 17:00 h (Universal Time). The environmental parameters inside the chamber were kept constant during the acclimation phase with CO₂ concentration entering the chamber of 400 μmol mol⁻¹, block temperature of 25°C, air flow of 300 μmol min⁻¹ and a PPFD of 800 μmol m⁻² s⁻¹ until the plant achieved a steady-state for stomatal conductance. Then the PPFD was lowered to 400 μmol.m⁻² s⁻¹ until the plant reached a new steady-state. After 10 minutes under this new steady-state, the PPFD was set back to its initial setting at 800 μmol.m⁻² s⁻¹. This allowed us to perform complete g_s response curves with stomatal closure kinetic followed by an opening kinetic. All the measurements were conducted on mature leaves grown from the third flush under control treatments. Each data point during the response curve was logged every 30s.

“steady state” data as mentioned in table E and through the manuscript were selected after stabilization of g_s (standard deviation of $g_s < 0.0025$ at each steady state), before and after each light change (SS1, SS2 and SS3). “-PPFD” suffix added to gas exchange parameters as mentioned in tables and in the manuscript refers to gas-exchange measurements extracted from the high light steady state SS1.

Dynamic model description

The stomatal responses of the irradiance curves were adjusted using a sigmoidal model based on Vialet-Chabrand et al. (2013) as modified by Gerardin et al. (2018). The sigmoidal model allows the estimation of parameters describing the temporal response of the stomata to an environmental change. The following equation was used:

$$g_s = g_0 + (G - g_0)e^{-e^{\left(\frac{\lambda-t}{\tau}\right)}}$$

Where g_s is the fitted stomatal conductance, g_0 is the starting value of the stomatal conductance (first steady-state obtained after the plant acclimation to the environmental conditions inside the Licor chamber), G the ending value of stomatal conductance (second steady-state reached after the full stomatal response to the irradiance change), λ is a time constant describing the lag time of the stomatal response (time needed to reach the inflection point of the curve from the moment of the irradiance change in each curve), and τ is another time constant describing the response through the steepness of the curve. From these parameters, the maximum slope (SL) as estimator of the speed of the stomatal response, has been calculated as:

$$SL = \frac{G_{end} - g_{start}}{\tau \cdot e}$$

τ is the response time and describes the steepness of the curvature, the lower a τ value is, the stronger the curvature and the higher SL will be, so the “faster” stomata will move. Whereas λ is the lag time of the stomatal response from the environmental change to the inflection point of the curve. Compared to the sigmoidal equation used by Vialet-Chabrand et al. (2013), here, λ is independent from τ and thus SL. For the adjusted parameters (λ , τ and SL) we also calculated the ratios of each parameter between the closing and opening sequences (λ_r , τ_r and SL_r , respectively), describing the degree of asymmetry of the light curves response. “-cl” and “-op” suffixes as mentioned throughout the manuscript refer to the parameters estimated from the closing and opening sequence respectively.

The amplitude of g_s variation (SA) was calculated as the difference between the mean steady-state at high irradiance (SS1 and SS3) and the steady-state at low irradiance (SS2) as either (SS1-SS2) or (SS3-SS2). The dynamic model was adjusted using the function “nlminb” of R (R Core Team 2015). To facilitate the adjustment of the sigmoidal model, five data points during the steady state before changing the irradiance were first included in the model adjustment. This impacts only the lag time λ , which was then corrected by subtracting the added time-period. The model adjustment is sensitive to

the starting point and including five steady state points allows the starting steady state g_s to be more robust as well as decreases the dependency of the adjustment on measurement noise.

Photosynthetic capacity

Photosynthetic capacity was estimated using the same portable photosynthesis system as described above (LI-COR 6400; LI-COR, Lincoln, NE, USA). All measurements were carried out between 09:00 and 18:00 h (Central European summertime). The environmental parameters inside the chamber were kept constant during the acclimation phase at 400 ppm CO₂, with temperature regulated at 25°C, flow at 300 and a photonflux density at 1000 $\mu\text{mol}\cdot\text{m}^{-2}\cdot\text{s}^{-1}$. All the measurements were conducted during three measurements campaigns, one on mature leaves from the second flush (F2, control conditions), one on mature leaves from the third flush (the same leaves as used for light response curves) before the beginning of water deficit treatments (F3) and the last campaign on the same flush and leaves as F3 after that plants were subjected to their respective treatment conditions setting (F3T). “-Aci” suffix added to gas exchange parameters as mentioned throughout the manuscript refers to gas exchange measurements extracted after plant acclimation to the conditions in the LI-COR chamber (described above) A/C_i curves were performed changing the [CO₂] entering in the chamber using the following sequence: 400, 300, 200 150, 100, 50, 0, 400, 400, 600, 800, 1000, 1200, 1500 and 2000 $\mu\text{mol mol}^{-1}$. Between each [CO₂] step, the leaves acclimated to new conditions for 2-3 minutes before logging..Aci curves were fitted using the “fitaci” function from the “plantecophys” Rstudio package based on the Farquhar-Berry-von Caemmerer model of photosynthesis and intercellular CO₂ concentration (Duursma, 2015) allowing the estimation of the maximal potential electron transport rate (J_{max}) and the maximum RubisCo activity (V_{max}).

Biomass measurements

Final harvest

At the end of the experiment, heights (H) and diameters (D) were measured then all the plants harvested. The branches (BBm), stems (SBm), leaves (FBm) were dried at 65°C until the sample reached a stable dry weight. The total plant leaf surface area was also measured (LS). Additionally, the woody biomass (WBm) and above ground biomass (AGBm) and leaf masse area (LMA) were also calculated (see table A for units and calculations).

The root biomass (RBm) has been measured for all the plants, and separated into the biomass for taproots (TRBm), coarse roots (CRBm) and fine roots (FRBm), where the fine roots were defined by diameters inferior to 1mm. Total roots other than taproots was also calculated (CFRBm = CRBm + FRBm). The tap roots were counted (TRn) and separated from the smaller roots (diameter <1cm). All

roots were dried at 65°C and weighted (balance type). The separation of coarse and fine roots was only done for 24 seedlings randomly chosen among the plants used for light curves, The proportion of CRBmr and FRBmr was calculated in regard to CFRBm, the ratio between coarse and fine roots ($R_r = \text{CRBm} / \text{FRBm}$) was calculated, and the proportion of TRBm was estimated relative to RBm. For each of the 24 seedlings for which fine roots were separated, a subsample was analysed using the WinRHIZO software (v. Pro 2009c, Regent Instrumentals, Québec, Canada) in order to determine the root mass area (RMA). This was then used to estimate the total plant fine root surface area (FRS) and then the root-leaf surface ratio (RSSr). From these biomass estimations the ratio between root and total shoot biomasses was calculated (RS) as well as the total dry biomass of the plants (TBm).

During the final harvest, per plant, two 3rd flush-leaves, close to the leaf used for gas exchange, were sampled from the 32 plants used for light curves to determine their relative water content (LRWC) as well as their osmolarity (Osm). These leaves had grown under the treatment conditions. These leaves were weighed (fresh mass MF) right after the harvest and then rehydrated in the dark for 24h. One leaf was used to measure the osmotic potential using a Vapour Pressure Osmometer (WESCOR 5500, Utah, USA), the other leaf was weighed at full turgor (MFT), dried at 65°C and reweighed (MD). The LRWC was estimated as $(\text{MF}-\text{MD})/(\text{MFT}-\text{MD}) \times 100\%$. In addition, the leaf of each plant used for gas exchange measurements was collected and split in half. One half was used for the analyse of nitrogen (N) and carbon (C) contents and carbon isotopic discrimination ($\delta^{13}\text{C}$). The other half was used to characterize the stomatal morphology (described below).

Stomatal morphology

At the end of the experiment all the leaves used for gas exchanges (one per plant) were sampled in order to determine the stomatal morphology. The following parameters were measured: the stomatal density (SD), the ostiole length (OL), the length of the stomatal guard cell complex (GCL), the ratio between the ostiole and guard cell lengths (SC: OL/GCL), guard cells width (GCW) and the stomatal size (SS: defined as an elliptical area $\pi \times (\text{GCL}/2) \times (\text{GCW}/2)$). Since both species only display stomata on the inferior surface of the leaves, 1cm² portions were collected and nail polish imprints were taken of the adaxial surface using adhesive film then applied on microscope slides for analysis. Stomata and epidermis cells were counted in the obtained pictures using the ImageJ2 software. Six (500*370µm) images were taken per plants and 10 stomata measured per pictures.

Transpiration efficiency estimation

To estimate TE, the total water consumption (TWC) of the plants has been measured by adding each watering cycle over a four months period from May to the final harvest in September In addition, the

water soil evaporation of 4 unplanted pots (2 control and 2 drought) has been measured and summed and the average water evaporation subtracted to the total water consumption of each plant.

Since the seedlings were 3 months old when the water consumption monitoring started, initial biomass had to be estimated.

The seedlings not selected by the screening of W_i (see above) were harvested and used to estimate the initial biomass (iBm) of the remaining plants at the start of water consumption monitoring. The heights were measured then the seedlings were harvested, dried and weighted resulting in the following allometry.

$$iBm = 0.025884 * (H^{0.9402055}) \quad r^2=0.92 \quad n=30$$

with iBm, the initial dry mass and H the height of the plants at the moment of the estimation.

At the beginning of the water consumption monitoring, the heights of the remaining plants were measured and their iBm estimated using this allometry. The actual biomass produced during the 4 months water monitoring period was estimated as $B_m = T_{bm} - iB_m$, and then TE was calculated as:

$$TE = (B_m / TWC)$$

Additionally, B_m and TWC were standardized to the final foliar surface area (B_mS and $TWCS$: table A)

Nocturnal and daily transpiration estimation

To estimate the nocturnal transpiration (NT) five weighting kinetics were performed based on hourly weightings for a whole day. The nocturnal period was defined by the nautical twilight for sunset and sunrise definitions resulting in the 23:00-4:00 period of measurement. However, it appeared from one night of hourly weightings that the stomatal opening did not occur before 5:00. We also tested if starting the period of measurements at 22:00 would have any significant impact on NT, which didn't. Thus, to increase precision, the data included in the calculation of NT covered an extended period between 22:00-5:00, whereas for the estimation of DT, the period 5:00-22:00 of the day before was used. As water losses estimations, the unplanted pots were used to correct the water evaporation from soil surface. The time separating each weighting was used to estimate a transpiration flux. Along each weighting kinetic, the daily transpiration (DT over 24h) including NT was also calculated and the proportion of NT over DT estimated (NDR). Similarly to B_m and TWC, the nocturnal and daily transpiration were standardised to the plants foliar surface (NTS and DTS, respectively).

Statistical analysis

All statistical analyses were performed with R (R Core Team (2015)). Treatments and species effects were analysed as a two-factorial design by analysis of variance (ANOVA). Significant differences were considered at $P < 0.05$. When the ANOVA found a significant treatments and/or species effect, a Post-Hoc test using Tukey-HSD test (package R, “agricolae”) was used to define inter-groups differences. To analyse the relationships between transpiration efficiency and its underlying traits, ANCOVA was used with treatment and species as fixed factors and a covariate. Partial R^2 for the covariate were estimated from Type I sum of squares for the covariate against the total sum of squares. p-values were adjusted for multiple comparisons using the “p.adjust” function with the “FDR” method

Results

Drought effect

Biomass traits

Overall most of the morphological traits were significantly affected by the drought treatment (Table 2). Globally, both species produced significantly less TBm under drought than control treatment which also translated in significantly lower RBm and AGBm under water stressed conditions. Despite such reductions in above and root biomass, the root/shoot ratio (RS) remained similar to the ones found in the control groups. However, the fine root surface to leaf surface ration (RLSr) decreased significantly under drought. In accordance with the globally reduced biomass, both species displayed significantly reduced LS and only tendencies for lower leaf biomass (LBm) which led to similar LMA between drought and control groups. Among the leaf related traits, the ratio between leaf and above ground woody biomass (FS) was the only one to significantly increase for both species under drought condition. In addition, both species displayed lower WBM under stress due to significantly reduced SBm and tendencies for lower values of BBm. Interestingly, all groups displayed similar heights (H), however, in both species, the diameter (D) was reduced under stress.

Similarly, to others morphological traits, almost all root related traits displayed significantly lower values under drought regardless of the species. Both species displayed lower RBm due to significantly lower CRBm and tendencies for lower FRBm which led to lower Rr under drought. TRn were similar inside each treatment, regardless of the species while TRBm was significantly lower under stress condition which along with the lower values of UGBm led to similar TRBmr between the groups.

Additionally, even though leaves had grown when treatment conditions were achieved, no so significant drought effect was found for the stomatal traits (OL, GCL, GCW, SC, SS, SD), however, both leaf nitrogen and carbon concentration were respectively found significantly and slightly increased under drought.

Physiology

Under drought conditions the steady-state gas exchange measurements (A_n , g_s) extracted from ACi and irradiance response curves were found significantly lower under drought for both species (Table 3), as was photosynthetic capacity (J_{max} , V_{max}). In addition, the daily transpiration (DT) as well as total water consumption per leaf surface (TWCS) were significantly lower under drought while NT was not affected by the drought.

Under drought condition, both species displayed significantly faster stomatal responses to irradiance changes, by displaying lower lag time (λ) as well as response times (τ). The lower τ resulted in significantly higher SL values under drought, even though SA also decreased significantly.

The reduced assimilation and stomatal conductance led to significantly higher intrinsic water use efficiency (W_i) under drought in both species also associated with significantly less negative values of isotopic composition ($\delta^{13}\text{C}$) in the leaves used for gas exchanges. Similarly, both species displayed significantly higher transpiration efficiencies (TE) under drought conditions linked to significantly reduced transpiration (TWC), even though also biomass growth was reduced (Bm) Despite such decrease in transpiration both species displayed same levels of LRWC regardless of the treatment (Table 2), while Osm was found significantly increased under drought condition.

Species differences and interaction with drought

Morphology

Both species displayed significant species effects on many variables (Table 2). Globally, regardless of the treatment, *Q. robur* produced more total biomass (TBm) than *Q. petraea*, which was mainly due to a higher root biomass (RBm) but also higher woody biomass (WBm), still resulting in significantly higher root/shoot ratio (RS) in *Q. robur*. The stronger growth in *Q. robur* was associated with higher diameters. However no significant difference was found for the mass of the acorns of the two species (4.3g for *Q. robur* and 4.1g for *Q. petraea*, t-test $P=0.41$), whereas a large variation of acorn masses were observed (1.7g to 8.1g). For leaf related traits, *Q. robur* showed significantly lower LMA and less leaves per above ground biomass (FS) than *Q. petraea*.

Most of the species differences were found for the underground biomass related traits. *Q. robur* produced systematically more RBm than *Q. petraea*. When divided in coarse and fine roots (CRBm and FRBm, respectively), *Q. robur* still displayed significantly higher biomass production for CRBm, while there was only a tendency for FRBm, resulting in significantly higher Rr in *Q. robur*. Additionally, both species produced similar TRBm, however *Q. petraea* produced a higher number of tap roots (TRn). These differences in coarse, fine and tap roots biomass led to significantly lower proportion of tap roots (TRBmr) in the underground biomass for *Q. robur* groups.

Moreover, no differences between species were found for the stomatal traits (OL, GCL, GCW, SC, SS, SD) as well as the nitrogen and carbon leaves concentration (N and C, respectively).

Overall, there were strong treatment and species effects on many morphological variables. The only interaction effect detected in the analysis of variance was related to the root biomass (RBm), *Q. robur* displaying more reduced RBm under drought than *Q. petraea*. However, the post-hoc analysis using

Tukey HSD test (Table 2) suggested some stronger drought responses of *Q. petraea* related to less fine root surface and biomass, as well as less coarse and tap root biomass, a lower fine root proportion but a higher leaf proportion, compared to *Q. robur*, which showed a significant reduction of overall root

Table 2: Morphological traits. Model wise p-values were adjusted for FDR and effect significances were only presented for models with p<0.05

	QPC	QPD	QRC	QRD	sp	ttmt	int
LS	4113,54 ± 286,87a	3258,42 ± 401,73a	4115,24 ± 194,8a	3574,93 ± 164,75a		*	
FRS	7229,6 ± 412,77a	3204,48 ± 307,39b	7849,34 ± 1088,54a	5122,37 ± 534,27ab		**	
RLSr	2,01 ± 0,27a	1,19 ± 0,22a	2,2 ± 0,29a	1,36 ± 0,19a		*	
LBm	29,61 ± 2,2a	23,49 ± 2,36a	25,26 ± 1,35a	23,45 ± 1,07a		.	
LMA	7,16 ± 0,18a	7,28 ± 0,21a	6,15 ± 0,18b	6,6 ± 0,2ab	***		
LRWC	90,42 ± 0,51a	92,62 ± 1,01a	91,67 ± 0,63a	91,2 ± 0,5a			
Osm	700,75 ± 16,51c	857,63 ± 13,71a	715,5 ± 37,52bc	794,25 ± 14,48ab		***	
BBm	9,75 ± 1,62ab	8,13 ± 1,39b	13,42 ± 1,32a	9,06 ± 0,99ab		.	
Bn	6,44 ± 1,15a	5,56 ± 1,3a	7,5 ± 1,43a	7,36 ± 1,83a			
RMA	2,63 ± 0,19a	3,98 ± 0,57a	2,85 ± 0,46a	3,97 ± 0,36a		*	
CRBm	31,11 ± 4,18a	14,97 ± 0,58b	43,45 ± 3,99a	32,72 ± 2,9a	**	**	
FRBm	18,79 ± 1a	12,75 ± 1,16b	19,92 ± 1,79a	19,59 ± 0,63a	.	.	
CFRBm	43,14 ± 3,77bc	32,94 ± 2,26c	86,34 ± 8,88a	54,15 ± 3,34b	***	***	*
CRBmr	61,45 ± 2,37b	54,4 ± 1,62c	68,49 ± 1,04a	62,14 ± 1,95ab	**	**	
FRBmr	38,55 ± 2,37b	45,6 ± 1,62a	31,51 ± 1,04c	37,86 ± 1,95bc	**	**	
Rr	1,63 ± 0,15b	1,21 ± 0,08b	2,2 ± 0,11a	1,67 ± 0,13b	**	**	
TRBr	40,73 ± 2,15a	39,24 ± 2,04a	25,1 ± 1,85b	30,65 ± 2,02b	***		
TRBm	28,77 ± 2,22a	20,94 ± 1,38b	26,97 ± 1,89ab	23,89 ± 1,97ab		*	
TRn	2,19 ± 0,37a	2,38 ± 0,29a	1 ± 0b	1,21 ± 0,11b	***		
RBm	71,9 ± 5,08bc	53,87 ± 2,67c	113,3 ± 9,43a	78,04 ± 3,72b	***	***	
SBm	44,69 ± 4,74a	25,04 ± 2,15b	47,64 ± 4,17a	36,73 ± 2,87ab		***	
WBm	54,44 ± 4,22ab	32,16 ± 2,2c	61,06 ± 3,64a	45,79 ± 2,59b	*	***	
AGBm	84,04 ± 5,9ab	55,65 ± 4,12c	86,32 ± 4,24a	69,24 ± 3,36b		***	
TBm	155,94 ± 9,4b	109,53 ± 5,99c	199,62 ± 11,33a	147,27 ± 5,69b	***	***	
RS	0,9 ± 0,07b	1,01 ± 0,06ab	1,34 ± 0,11a	1,15 ± 0,07ab	**		
FS	0,56 ± 0,04b	0,74 ± 0,05a	0,43 ± 0,03b	0,52 ± 0,02b	***	**	
BSr	0,34 ± 0,13a	0,34 ± 0,07a	0,35 ± 0,06a	0,27 ± 0,04a			
H	135,07 ± 13,94a	103,03 ± 6,9a	132,08 ± 11,04a	130,85 ± 11,62a			
D	12,09 ± 0,58ab	10,53 ± 0,32b	13,23 ± 0,42a	12,05 ± 0,4ab	*	**	
OL	14,03 ± 0,2a	13,77 ± 0,38a	13,81 ± 0,3a	13,98 ± 0,3a			
GCL	25,87 ± 0,35a	26 ± 0,6a	26,68 ± 0,47a	26,42 ± 0,38a			
GCW	18,09 ± 0,25a	18,38 ± 0,37a	18,76 ± 0,27a	18,41 ± 0,18a			
SC	54,32 ± 0,8a	52,96 ± 0,49a	51,77 ± 0,56a	52,94 ± 0,89a			
SS	368,1 ± 9,12a	376,53 ± 14,55a	393,53 ± 11,88a	382,06 ± 7,79a			
SD	555,13 ± 24,51a	621,25 ± 33,91a	586,13 ± 20,68a	535,63 ± 40,55a			
N	1,72 ± 0,12b	2,32 ± 0,11a	2,09 ± 0,08ab	2,25 ± 0,12a		**	
C	45,34 ± 0,65b	45,59 ± 0,33ab	45,55 ± 0,22ab	47 ± 0,19a		.	

biomass under drought as well as a lower coarse to fine roots ratio. It needs to be noted, however, that the separation of coarse and fine roots was based on a lower sample number than TRBm, CFRBm and TRBm, these results need to be interpreted with caution. Post-hoc tests also suggested for *Q. petraea* a higher osmotic adjustment and more leaf nitrogen under drought.

Physiology

No difference between species was found for the steady state gas exchange measurements (A_n , g_s) extracted from both ACi and irradiance response curves when hydric regimes were applied (Tables 3, 5), despite a slight tendency for higher assimilations values in *Q. robur*. The same results were found for the photosynthetic capacity, both species displaying similar J_{max} and V_{max} values inside each treatment. Similar nocturnal (NT) and diurnal transpirations (DT) were found in both species, NT accounting for about 6% of the daily transpiration.

Table 3 : Means per groups (\pm SE) of water use estimators and their components, with the Assimilation (A_n), the stomatal conductance (g_s), intrinsic water use efficiency ($W_i = A_n/g_s$) of light curves and A-ci curves at high irradiance steady-state values (PPFD and A_{-ci} respectively), the transpiration efficiency (TE), the water consumption (TWC), the biomass accumulation of the plant (Bm) and the isotopic discrimination ($\delta^{13}C$). Different letters show the significative differences among groups from the ANOVA model including treatments and species effects followed by a post-hoc Tukey test. Overall species (SP), and treatment (T) and interaction effect (SP*T) are presented as is: (P values: "****" for $P < 0.001$; "***" for $P < 0.01$; "**" for $P < 0.05$). Model wise p-values were adjusted for false discovery rate ("fdr" method) and effect significances were only presented for significant models with $p < 0.05$.

	QPC	QPD	QRC	QRD	SP	T	SP*T
Wi PPFD	93,1 \pm 9,44a	124,87 \pm 11,86a	86,85 \pm 6,55a	130,19 \pm 17,51a		*	
A_n PPFD	10,51 \pm 1,17b	5,63 \pm 0,72c	14,74 \pm 1,04a	5,84 \pm 0,7c	.	***	*
g_s PPFD	0,12 \pm 0,02ab	0,05 \pm 0,01b	0,18 \pm 0,03a	0,05 \pm 0,01b		***	
Wi Aci	89,48 \pm 9,43b	123,78 \pm 7,82a	85,69 \pm 3,3b	133,29 \pm 11,05a		***	
A Aci	12,07 \pm 1,61a	5,62 \pm 0,89b	14,21 \pm 1,34a	6,08 \pm 1,05b		***	
g_s Aci	0,15 \pm 0,03a	0,05 \pm 0,01b	0,17 \pm 0,02a	0,05 \pm 0,01b		***	
TE	4,07 \pm 0,15c	5,23 \pm 0,16a	4,62 \pm 0,14b	5,4 \pm 0,14a	*	***	
TWC	37,03 \pm 2,12a	20,31 \pm 0,84b	40,93 \pm 2,15a	26,52 \pm 1,00b	*	***	
Bm	153,9 \pm 9,54b	107,94 \pm 5,26c	197,83 \pm 11,53a	143,03 \pm 6,02b	***	***	
TWCS	9,37 \pm 0,49a	6,63 \pm 0,39b	9,99 \pm 0,41a	7,52 \pm 0,28b		***	
BmS	37,37 \pm 1,48b	33,99 \pm 2,3b	47,26 \pm 1,83a	40,08 \pm 1,62b	***	*	
NT	21,8 \pm 3,75a	19,73 \pm 3,09a	20,13 \pm 2,34a	22,14 \pm 2,26a			
DT	368,46 \pm 30,27ab	288,29 \pm 25,98b	428,69 \pm 19,09a	343,62 \pm 18,83ab	.	**	
NDr	6 \pm 0,63a	6,77 \pm 0,69a	4,89 \pm 0,47a	6,34 \pm 0,56a			
NTS	0,05 \pm 0,01a	0,06 \pm 0,01a	0,05 \pm 0,01a	0,06 \pm 0,01a			
DTS	0,93 \pm 0,08a	0,95 \pm 0,04a	1,06 \pm 0,04a	1,02 \pm 0,04a			
$\delta^{13}C$	-27,88 \pm 0,52ab	-26,87 \pm 0,31a	-28,22 \pm 0,36b	-27,33 \pm 0,14ab		*	
V_{max}	49,33 \pm 7,03a	41,32 \pm 8,03a	64,16 \pm 6,71a	36,66 \pm 7,35a		*	
J_{max}	85,95 \pm 10,3ab	53,41 \pm 12,7b	114,19 \pm 12,06a	62,46 \pm 13,34b		**	

Within each treatment, both species displayed the same dynamic responses for all the parameters (τ , λ and SL) for both closing and opening sequences (Table 4). However, a few differences appeared while comparing both sequences, for τ both species only displayed tendencies for slower responses during the opening sequence, while for λ , only *Q. robur* displayed significantly slower opening than closing. Similarly to the other two parameters when found significant, the response was faster (lower SL values) during opening than closing for both species at the exception of the « QPC » group. Additionally, no difference was found between species for the amplitude of response to irradiance for the two sequences in both, absolute (SA) and relative terms (RSA) and both closing and opening sequences displayed similar amplitudes.

Table 4 : Kinetics parameters for opening and closing sequences (means \pm SE), with τ the response time (sec), λ the delay of stomatal response to reach the inflection point (sec), SL the maximal slope of the response and the amplitude of variation (closing SS1-SS2 and opening SS2-SS3) of the parameters between each steady state (SA and RSA (%)), respectively in absolute values and percentage). Different letters show the significative differences between groups from the ANOVA model including treatment and species effects performed on closing and opening sequences separately and followed by a post-hoc Tukey test. ($n = 4-8$ repeated measurements per group). The significant differences between the opening and closing sequence computed by a paired t-test are presented as is (P values: “***” for $P < 0.001$; “**” for $P < 0.01$ and “*” for $P < 0.05$), so a significative difference indicates an asymmetric response.

		closing		opening	Cl/op
QPC		309 \pm 66a	.	296 \pm 26ab	0,68 \pm 0,01a
QPD	τ	121 \pm 20c	ns	147 \pm 31b	0,91 \pm 0,11a
QRC	(sec)	227 \pm 23ab	.	359 \pm 73a	0,75 \pm 0,13a
QRD		131 \pm 9bc	.	212 \pm 36ab	0,68 \pm 0,1a
	SP				
	T	***		*	
QPC		395 \pm 58a	.	395 \pm 42ab	0,77 \pm 0,14a
QPD	λ	131 \pm 15b	ns	137 \pm 16b	0,96 \pm 0,05a
QRC	(sec)	367 \pm 41a	*	518 \pm 86a	0,76 \pm 0,07a
QRD		169 \pm 17b	*	225 \pm 31b	0,8 \pm 0,11a
	SP			*	
	T	***		***	
QPC		4,5 \pm 0,18a	ns	3,9 \pm 0,15a	1,62 \pm 0,18a
QPD	SL	7,3 \pm 0,17a	*	4,0 \pm 0,12a	1,98 \pm 0,32a
QRC	($\mu\text{mol m}^{-2} \text{s}^{-2}$)	9,6 \pm 0,17a	**	5,9 \pm 0,16a	1,95 \pm 0,33a
QRD		5 \pm 0,14a	*	3,7 \pm 0,15a	1,91 \pm 0,36a
	SP				
	T				
QPC		0,03 \pm 0b	ns	0,03 \pm 0,01ab	
QPD	SA	0,02 \pm 0b	ns	0,01 \pm 0b	
QRC	($\text{mol m}^{-2} \text{s}^{-1}$)	0,06 \pm 0,01a	ns	0,05 \pm 0,01a	
QRD		0,02 \pm 0b	ns	0,02 \pm 0,01ab	
	SP				
	T	**		*	
QPC		-26,68 \pm 3,66a	ns	-23,07 \pm 1,12a	
QPD	RSA	-39,08 \pm 2,81a	ns	-28,04 \pm 2,97a	
QRC	(%)	-32,92 \pm 3,9a	ns	-29,62 \pm 5,53a	
QRD		-30,61 \pm 2,97a	ns	-28,83 \pm 3,66a	
	SP				
	T				

Additionally, over the water consumption monitoring period, *Q. robur* transpired significantly more water (TWC) and produced more biomass (Bm) than *Q. petraea* regardless of the treatments. The differences in Bm and TWC led to significantly higher transpiration efficiency values for *Q. robur* in both treatments, but under drought treatment this difference was slightly smaller (Table 3).

The similar gas exchange measurements led to similar intrinsic water use efficiency (Wi) between the two species inside each treatment. In addition, both species displayed no differences for isotopic discrimination in the leaves used for gas exchanges ($\delta^{13}\text{C}$).

Decomposing WUE efficiency in components

All correlations were based on an ANCOVA, taking into account species and drought effects (see Table 5). These correlations are therefore independent from species or treatment induced variations and represent overall plant functioning of these oaks. Between the two components, TE did not correlate with TWC, but only positively with biomass increase (Bm) and by extent most of the biomass traits. Both components (Bm and total water consumption TWC) displayed significant correlations with each other. Most of the biomass traits correlated positively with Bm, however clearly most of the total biomass variation was explained by fine and coarse root biomass, followed closely by leaf biomass and surface. Similarly, TWC positively correlated with most of the biomass traits, displaying the highest values for TBm ($R^2 = 0.28$) and CRBm ($R^2 = 0.28$) as well as displaying high values for leaves related traits such as LBm and LS ($R^2 = 0.17$ and 0.21 , respectively). It is also worth to notice that none of the stomatal morphological features correlated with any of TE components traits nor TE itself. However, bulk leaf $\delta^{13}\text{C}$ negatively correlated with both TWCS and DTS ($R^2 = 0.23$ and 0.22 , respectively) while positively correlating with LBm and LMA ($R^2 = 0.16$ and 0.21 , respectively). Among physiological traits, the only significant correlation detected for gas exchange measurements was found between TE and Wi-PPFD at SS2 ($R^2 = 0.07$). TE displayed a stronger correlation with the time integrated estimator of Wi, the bulk leaf $\delta^{13}\text{C}$ ($R^2 = 0.29$). Additionally, no correlation was found for the photosynthetic capacity traits and only a few tendencies were detected for dynamics traits ($0.05 < P \text{ values} < 0.1$), TWC showing a small positive correlation with τ_{cl} ($R^2 = 0.05$), BmS displaying a small negative correlation for SL_{cl} ($R^2 = 0.14$), SL_{op} correlating with Bm and BmS ($R^2 = 0.1$ and 0.17 , respectively) while SLr displayed the only significant positive correlation with TWC ($R^2 = 0.08$) as well as a positive tendency for Bm ($R^2 = 0.19$). Total water consumption (TWC) was clearly driven by daily water consumption (DT: $R^2 = 0.23$), however variation in nocturnal transpiration also played a smaller significant role (NT: $R^2 = 0.07$). These correlations were also found when standardized to the leaf surface with DTS, TWCS and BmS both correlating positively with the latter ($R^2 = 0.25$ and 0.18 , respectively). In addition, both TWC and Bm were negatively correlated with leaf nitrogen N ($R^2 = 0.12$ and 0.08 , respectively).

	model TE	model TWC	model TWCS	model Bm	model BmS	model $\delta 13c$
TWCS	(-)0.07*				(+)0.33***	(-)0.23 *
BmS	(+)0.06*		(+)0.26***	(+)0.04.		
TE			(-)0.07*	(+)0.16***	(+)0.08*	(+)0.41 ***
TWC				(+)0.38***		
Bm	(+)0.16***	(+)0.25***			(+)0.05.	(+)0.08.
LS		(+)0.21***	(-)0.16***	(+)0.25***	(-)0.13**	
FRS				(+)0.19.	(+)0.18.	
RSLr					(+)0.36*	
LBm	(+)0.06*	(+)0.17***	(-)0.15***	(+)0.27***	(-)0.07*	(+)0.16 *
LMA	(+)0.09**			(+)0.05.	(+)0.06*	(+)0.21 *
SLA	(-)0.1**			(-)0.07.	(-)0.06*	(-)0.25 **
LRWC						
Osm	(+)0.07*			(+)0.1.		
SBm		(+)0.05*		(+)0.05.		
BBm		(+)0.04*	(-)0.05*	(+)0.08**		(+)0.13.
CRBm		(+)0.28**		(+)0.42***		
FRBm		(+)0.19*		(+)0.34***		
CFRBm	(+)0.13***	(+)0.13***		(+)0.3***	(+)0.09*	
CRBmr		(+)0.1.				
FRBmr		(-)0.1.				
Rr		(+)0.09.				
TRBm	(+)0.03.	(+)0.07**		(+)0.12***		
TRn						
RBm	(+)0.14***	(+)0.17***		(+)0.38***	(+)0.11**	
WBm	(+)0.04*	(+)0.16***		(+)0.2***		
AGBm	(+)0.06*	(+)0.21***		(+)0.28***		(+)0.11.
TBm	(+)0.16***	(+)0.28***		(+)0.51***	(+)0.15	
RS	(+)0.03.				(+)0.12**	(-)0.15 *
FS			(-)0.19***		(-)0.17***	
H		(+)0.03.		(+)0.05.		
D	(+)0.06*	(+)0.06**		(+)0.09**		
$\delta 13c$	(+)0.29***		(-)0.18*	(+)0.07.		
N		(-)0.12*		(-)0.08.		
C						
Vmax						
Jmax						
SL _{cl}					(-)0.14.	
τ_{cl}		(+)0.05.				
λ_{cl}						
τ_{op}						
SL _{op}				(+)0.1.	(+)0.17.	
λ_{op}						
τ_r						
λ_r						
SL _r		(+)0.08*		(+)0.19.		
Wi- PAR (SS2)	(+)0.07*					
NT		(+)0.07**		(+)0.07.		
DT		(+)0.23***		(+)0.24***		
NTS						
DTS	(-)0.06*		(+)0.25***		(+)0.18***	(-)0.22 *

Table 5: Major ANCOVA results obtained by models testing $\delta^{13}C$, TE and its components (TWC, Bm, TWCS, BmS) against morphological and physiological traits. Including the correlations sign, partial R^2 of the covariate and its P-value: “***” for $P < 0.001$; “**” for $P < 0.01$; “*” for $P < 0.05$ and “.” for $0.1 > P > 0.05$. (see annexe X or supplementary data for full table) With: $lm(\text{Model variable} \sim \text{Treatment effect} + \text{Species effect} + 1 \text{ covariate})$

Discussion

Drought impact on morphological traits

In the present study we aimed to characterize the impact of a severe drought on oak growth. As expected, under drought conditions, both species displayed a commonly reported response by producing globally less biomass in both above and belowground compartments (Bréda et al. 2008). Nevertheless, fine root biomass proportion relatively increased under drought, in relation to coarse roots in both species. As such a drought response of root biomass allocation has been observed before (Guehl et al. 1994), it might enhance drought tolerance by providing an improved access to soil water supply. Despite these decreased biomass productions in the drought treatment, height growth was not affected, whereas diameter growth was significantly reduced. Both, stomatal conductance and assimilation were reduced by more than 50 % in the drought treatment, probably limiting overall carbon availability in these young seedlings for growth, especially as the available LS was also less under drought. As the drought effect on photosynthetic capacity was small, the reduction in assimilation was probably rather due to an increased stomatal limitation. However, both species displayed a significant osmotic adjustment under this severe drought, maintaining the leaf relative water content at levels similar to non-stressed seedlings.

Species differences in morphological traits

Additionally, we explored the differences between the two oaks species susceptible to explain their respective ecological requirements. Most of the interspecific differences were found for root related traits both under control conditions and in response to drought. The root biomass (including both coarse and fine roots) appeared to be the only biomass traits for which the species displayed different responses to drought. Although, *Q. robur* systematically displayed higher root biomass production, it was more strongly reduced under drought than for *Q. petraea*. Despite similar above ground biomass observed in both species within each treatment, under control conditions *Q. robur* invested more in the root system than *Q. petraea* which, at first glance might seem in discordance with the latter known higher tolerance to drought, as efficiency of trees in terms of water relations depends on their ability to absorb water at rates allowing the avoidance of internal hydraulic failure due to a high evaporative demand (Bréda et al. 2008). By dissecting root biomass into coarse and fine roots we were able to show that *Q. petraea* produced proportionally more fine roots than coarse compared to *Q. robur*. This resulted in a similar fine root biomass as well as fine root surface in both species. Furthermore, both

species displayed interspecific differences for taproots, as most *Q.petraea* seedlings produced several taproots, whereas *Q.robur* seedlings very rarely had more than one. However, the overall biomass invested into tap roots was not different between the species. These results suggest that carbon allocation in seedling root systems is invested in a more efficient way by *Q. petraea* in term of water uptake by fine roots than *Q.robur*, thus compensating for the lower overall root biomass, but perhaps also providing an improved soil exploration due to several tap roots. Moreover, root traits displayed a different plasticity to drought in both species, therefore the soil-to-root interface might constitute a key component in the drought tolerance of the two oaks species. However, contrasting results were also reported in young oaks trees for which root growth was unaffected by two progressive severe droughts with rewatering while shoot and stem growth substantially declined (Arend et al. 2013). Such difference might be attributable to the severe drought applied in our study as well as the different experimental designs especially in term of available soil volume of root prospection. The differences in root traits between the two species observed in our study might suggest more complex and ramified root system by *Q. petraea* compared to *Q. robur* from an early stage of development which is in agreement with previous results which observed an increase in the root-leaf ratio under moderate drought in both species (Thomas & Gausling, 2000) as well as under severe drought in young sessile oaks (Thomas, 2000). This suggest that the differences in the structure of the root systems found between the two species might partly explain the observed difference in ecological niche of *Quercus* species (Dickson & Tomlinson 1996; Thomas et al. 2000).

Nocturnal and diurnal transpirations

To improve our understanding about the overall water consumption in oaks trees, we monitored their water loss over a daily course. As expected, under drought the seedlings consumed less, presumably due to the lower stomatal conductance as well as lower leaf surface which was positively correlated with TWC. Both species displayed similar nocturnal transpiration (NT) in both treatments. This might indicate that in oaks seedlings, no acclimation mechanism allows to reduce nocturnal water loss under stress. During night the cuticular conductance contribute to water loss, however, a significant nocturnal stomatal conductance has often been detected in numerous species (Zeppel et al., 2010) as well as among oaks species (Violet-Chabrand PhD thesis, 2013). Such water loss occurring at night might constitute a considerable cumulative water loss, especially for adult trees as we estimated NT to account for ~6% of the total daily water consumption, when summer nights represented only about five hours. Such results are comparable to previous night time transpiration values observed in oaks seedlings which were quite substantial by ranging from 4 to 33% of day time values (Violet-chabrand PhD thesis, 2013) thus confirming that in seedling the maintenance of open stomata during the night might play an important contribution to the plant water budget (Dawson et al. 2007).

Stomatal dynamics and morphology in response to drought

Another aim of our study was to assess the plasticity of the stomatal dynamic response to drought. Light is considered as the main driver of photosynthesis and stomatal conductance changes under natural conditions (Shimazaki et al. 2007). Therefore, we explored stomatal temporal responses induced by a decrease followed by an increase in irradiance displayed by oaks seedlings. Both species clearly showed faster dynamic responses under drought. Previous studies on stomatal dynamic recorded similar faster responses under water limited environments (reviewed by Vico et al. 2011; Tobacco: Gerardin et al. 2018), sometimes associated with increased transient water use efficiency (rice: Qu et al. 2016) as modelled by Lawson and Blatt (2014). Such faster stomatal responses have been hypothesized to translate water conservative behaviours (Vico et al. 2011; Lawson and Blatt 2014; McAusland et al. 2016) as faster closing might lead to an improved coupling between A_n and g_s , thus ultimately higher W_i . Moreover, there was a clear asymmetrical response to irradiance for all three dynamic parameters in both species, characterized by a faster closing which remained unchanged under drought treatment. Symmetry of dynamic response to irradiance has rarely been reported in literature, although it has been suggested that asymmetrical responses might contribute to water loss as well as CO_2 uptake (Ooba & Takahashi 2003; Lawson et al. 2010, 2012; Vialet-Chabrand et al. 2013; McAusland et al. 2016). Faster closing than opening would be associated with a water conservative behaviour (Tinoco-Ojanhuren & Pearcy, 1993) and has been recorded among various species (McAusland et al. 2016). Recently, Gerardin et al. (2018) highlighted a plasticity to drought in *Nicotiana tabacum* for the degree of symmetry in response to irradiance either accentuated or reduced depending on the dynamic parameter. Such results are in contradiction with the present stomatal behaviours expressed by oaks seedlings, thus hinting for species-specific behaviours in drought acclimation regarding stomatal opening and closing processes.

In many species stomatal morphology has been shown to be impacted by growth conditions (Casson and Gray 2008; Kardiman and Raebild 2018; Gérardin et al. 2018). However, in our study stomatal morphology of the used third flush leaves were not significantly changed by the drought treatment, which is in accordance with Guehl et al. (1994) for stomatal density in *Q. petraea*. Stomatal morphology has been linked to the rapidity of stomatal response. It has been observed that stomatal features could be associated with faster dynamic response which in turn might be associated with higher water use efficiency (Hetherington & Woodward 2003; Drake et al. 2013; Raven 2014). Various studies established clear variations among species for such stomatal dynamics traits and stomatal features such as stomatal size and density (McAusland et al. 2016). Interestingly, we observed no drought effect for any stomatal morphological traits. Therefore, the faster responses observed under drought stress cannot be attributed to changes in stomatal morphology. Hence, we assume that the

observed variability in dynamics among individuals as well as treatments might rather rely on physiological processes such as ion transport activity (Lawson and Blatt 2014) or Cl^- -mediated stomatal responses (Buckley et al. 2013) as previously proposed in species with elliptical shaped guard cells (Hetherington & Woodward 2003; Franks & Beerling 2009; McAusland et al. 2016).

Species differences for stomatal dynamics

For none of the stomatal dynamic traits a significant species difference could be detected and also no species to treatment interaction, suggesting that in terms of rapidity of stomatal reactions to changes in irradiance *Q. robur* and *Q. petraea* show similar behaviours, while a within species and inter leaf variability exists. We observed also no difference between the two species for stomatal morphology related traits.

Species differences in W_i and WUE, gas exchange

Overall the gas exchange measurements were comparable to previous studies performed on the two oaks species (Ponton et al. 2002; Epron and Dreyer 1993; Steinbrecher et al. 2013) and suggested that both species displayed highly similar assimilation rates as well as stomatal conductance in control as well as in drought conditions, with some exceptions. *Q. robur* displayed slightly higher assimilation rates and stomatal conductance under well irrigated conditions as well as a stronger decrease in assimilation rate under drought compared to *Q. petraea*. However, the photosynthetic capacity was not significantly different between the species. This could suggest a stronger drought impact on carbon assimilation via stomatal limitations in *Q. robur* seedlings, which could influence plant growth and survival in field grown trees. When detected, these small differences between species were in accordance with previous works also showing higher stomatal conductance and assimilation rate for *Q. robur* (Epron and Dreyer 1993; Ponton et al. 2002). However, in these two studies, the observed differences in gas exchange led to significantly higher W_i for *Q. petraea*, which was not the case in our study.

Interspecific variability in water use efficiency and $\delta^{13}\text{C}$.

In the present study, due to similar assimilation rates and stomatal conductance, the species displayed similar intrinsic water use efficiencies within each treatment. Nevertheless, it was clear that the stomatal conductance was the main driver of W_i variability rather than carbon assimilation in both species as well as under both hydric treatments. This confirms the previous results obtained in these oaks species attributing most of W_i variability to g_s (Roussel et al. 2009a, 2009b; Ponton et al. 2001), hence stressing the importance of stomatal regulation in gas exchange balance. In addition, similarly to the direct W_i estimations, also for bulk leaf $\delta^{13}\text{C}$ measurements no significant species difference was

detected. Our results do therefore not corroborate the higher W_i observed for *Q. petraea* recorded on mature trees originated from the same natural stand (Epron and Dreyer, 1993) or $\delta^{13}C$ (both in wood cellulose and leaves) measured in neighbouring trees (Ponton et al. 2001) or seedlings from pure stands in the same forest under control conditions (Ponton et al. 2002). Nevertheless, it is worth mentioning that these experimental designs were slightly divergent from the approach chosen in our experiment, as we grew seedlings originated from typical *Q. robur* or *Q. petraea* pure stands within a same provenance region and conducted a preliminary phenotypic screening on a larger number of individuals, thus maintaining a maximum W_i variability in the measured seedlings.

Transpiration efficiency

One of our main objectives was to study water use efficiency integrated at different levels, thus in addition to W_i and $\delta^{13}C$ measurements we monitored the water consumption as well as biomass production of the plants throughout the experiment, allowing us to estimate the whole plant transpiration efficiency (TE). To the authors knowledge, this was the first attempt to study drought as well as species differences for TE in *Q. robur* and *Q. petraea*. The transpiration efficiency values found in this study ranged from ~ 4.1 g DM L⁻¹ to 5.4 which are similar to observations found by Roussel et al. (2009) in *Q. robur* seedlings for which TE covered a range from 4.8 to 5.5 g DM L⁻¹. Scaled up TE at the whole plant level is indeed rarely seen in literature as its estimation is a laborious process integrating measurements over a long period (Roussel et al. 2009; Cernuzak et al. 2007, Guehl et al., 1994). In addition, as transpiration efficiency does not necessarily reflect leaf gas exchange performed by plants, upscaling from W_i to TE is not straightforward. Indeed, various processes such as respiratory carbon losses, production of volatile carbonated compounds and non-photosynthetic loss of water are likely to induce a discrepancy between these two WUE estimators (Farquhar & Richards, 1984). For instance, in our study, nocturnal transpiration accounted for $\sim 6\%$ of the daily water consumption regardless of the species and treatments. Nevertheless, in agreement with the sampling strategy and following the same trend than W_i and $\delta^{13}C$, transpiration efficiency significantly increased under drought for both species.

Species differences

The only significant WUE difference observed between *Q. robur* and *Q. petraea* was found in transpiration efficiency for which *Q. robur* displayed higher values than *Q. petraea*, especially under non-stressed condition, no significant difference was found for either $\delta^{13}C$ or W_i . This difference in TE was mainly due to the greater biomass production of *Q. robur* seedlings in both treatments. Nevertheless, most of the studies assessing oaks growth often described higher growth rates observed in *Q. robur* mature trees and seedlings compared to *Q. petraea*.

The theoretical relationship between W_i and $\delta^{13}C$ has been confirmed experimentally in various studies on oaks (Guehl et al. 1994; Picon et al. 1996; Ponton et al. 2002; Roussel et al. 2009). We detected a significant correlation between leaf level integrated intrinsic water use efficiency ($\delta^{13}C$) and TE, which suggests that partly the whole plant TE still depends on g_s , as variations in W_i were more strongly determined by g_s than A_n . Our results demonstrated that upscaling from intrinsic water efficiency to whole plant transpiration efficiency might not always be straightforward. Indeed, the similar W_i as well as $\delta^{13}C$ variations found among species inside each treatment were not repeated for transpiration efficiency, for which *Q. robur* displayed significantly greater values. W_i is measured either under standardized conditions or is an instantaneous snapshot of plant functioning, which might not be representative of the combined functioning of all leaves. However, already the temporal integration at “one leaf level” using $\delta^{13}C$ showed that a higher leaf level W_i could explain part of the higher whole plant TE. We also only detected a single relationship between low irradiance steady states W_i (W_i -PPFD SS2) and TE. Such observation could suggest that low irradiance gas exchanges were more representative of the plant gas exchanges integrated over the whole TE monitoring than high irradiance steady states. Although Roussel et al. (2009) previously established a strong relationship between W_i and transpiration efficiency measured the on the same day in a *Q. robur* full sib family, our results hinted toward the fact that steady states W_i , although being similar at low and high irradiance, were not representative of integrated gas exchanges throughout the experimentation. Thus, leading to the observed discrepancy between W_i and the other two WUE estimators. Brendel et al. (2008), whom also found low correlations between $\delta^{13}C$ and W_i obtained in field measurements, suggested that environmental influence on gas exchange might induce noise in W_i estimation leading to the weak relationships. Such discrepancy between whole plant water use efficiency and intrinsic water use had already been observed in *Q. robur*, the two traits were reported as uncoupled (Guehl et al. 1995). Despite the contrasting results observed between various WUE estimators, bulk leaf $\delta^{13}C$ proved itself as a reliable proxy for TE, as ANCOVA models detected relatively high correlations between the two traits ($R^2 = 0.29^{**}$ and 0.41^{***} : see table 5). Such findings suggest that leaf isotopic discrimination ($\delta^{13}C$) might be used instead of transpiration efficiency in future large screening experiments, avoiding the particularly constraining and time consuming TE estimation.

Correlations : biomass traits and TE (components)

Overall, transpiration efficiency variations were driven directly by the biomass accumulation rather than water use throughout the experiment, while the biomass itself was mostly depending on underground biomass traits. In addition, water use was positively correlated to the total plant biomass and especially leaves surface and biomass. Therefore, even though W_i was mainly driven by stomatal conductance stressing the importance of stomatal regulation on gas exchange, once upscaled to whole

plant, the biomass setting the transpiring leaf area plays a determinant role in TE. Furthermore, neither the accumulated biomass or water use correlated with A_n or g_s , respectively. For instance, Li et al. (2011) reported carbon loss reaching up to 25% of assimilation rates re-emitted as isoprene in *Q. robur* leaves submitted to heat stress. Thus, one cannot exclude that an intra-specific variability in these processes might be involved in the observed TE differences between the two species (Steinbrecher et al. 2013).

To our knowledge, this study was the first comparing stomatal morphology between *Q. robur* and *Q. petraea*. For *Q. robur*, stomatal density had been linked within a full-sib family to the variability of intrinsic water use efficiency, probably through the expression of gene ERECTA and its impact on stomatal density and size (Roussel et al. 2008). However, the lack of correlations (ANCOVA) between $\delta^{13}C$ and stomatal morphology that we found for both species regardless of the treatments does not corroborate such a relationship or at least suggest that there was an insufficient stomatal density variability in our populations to detect any correlation.

Correlations dynamic

In this study we were unable to link the dynamics parameters significantly with transpiration efficiency or its components (TWC and Bm), when accounting for species and treatment differences. However, establishing such relations might be difficult on the within species level, where variations in stomatal speeds might not be sufficient to impact the whole plant growth and water use. Also, single leaf measurements of stomatal dynamics were performed, which might not accurately represent the whole plant functioning. Such experiments tend to point out that one single leaf dynamic properties are in fact unlikely to reflect the dynamics of the whole plant at a given point in time. Therefore, further studies are needed to understand the temporal response of oaks seedlings to environmental changes to accurately estimate a whole plant dynamic state eventually linkable with long-term gas exchange integrations.

Conclusion

Using seedlings of *Q. robur* and *Q. petraea* originating from natural pure stand, we showed that both species displayed highly similar responses to drought characterized by the similar levels of gas exchanges and the same faster dynamics to transient irradiance. Most of the detected differences between the two species were found in their biomass allocation, especially in the root related traits which indicated the establishment of a more ramified root system by *Q. petraea* possibly linked to a better tolerance to drought and a higher soil prospection capability. On the other hand, *Q. robur* distinguished itself from *Q. petraea* by producing globally more biomass which is in accordance with its pioneer attribute often described. In contradiction with most of the literature, no differences

between species for intrinsic water use efficiency were detected. However, for the first time we showed greater transpiration efficiency in *Q. robur* than *Q. petraea* seedlings. In addition, the expected relationship between W_i and $\delta^{13}C$ was respected. Furthermore, $\delta^{13}C$ and TE displayed a relatively tight correlation with each other which led us to conclude that steady state gas exchange were not representative of a time integrated water use efficiency. Nevertheless, we confirmed previous works proposing stomatal conductance as the main W_i driver in oaks and highlighted the importance of biomass production and leaf surface on TE variability. However, we were unable to link temporal response dynamics to irradiance as well as stomatal anatomy with the latter. Which, altogether with the observed discrepancy suggest that a huge part of the mechanisms involved in TE diversity remains unveiled.

Our study suggested different strategies in root development displayed by both species from a young age, exploring these differences in field and assessing whether these strategies are maintained by older trees might greatly improve our understanding of species differences as well as mechanism involved in their respective drought tolerance. In addition, little is known about dynamics under transient irradiance. The faster responses displayed by both species although not linked to TE nor water consumptions hinted toward an acclimation of dynamics to drought. Hence further studies using different irradiance steps might contribute to assess a potential key role of dynamics in drought tolerance and water balance.

Declaration of interest

All authors disclose any financial or personal conflict of interest.

Author contributions

OB and DLT designed the experiment, OB provided study material and environment, TG, and OB conducted the experiment, TG, OB did the data analysis, and TG, OB and DLT wrote the manuscript and were involved in the interpretation and critical discussion of the results, OB obtained funding.

Acknowledgements

TG acknowledges the PhD grant from the H2Oak ANR-14-CE02-0013 project. This study was part of the interdisciplinary « H2Oak » research project aiming to investigate the diversity for adaptive traits related to water use in two European white oaks (*Quercus robur* and *Quercus petraea*). The UMR Silva is supported by the French National Research Agency through the Laboratory of Excellence ARBRE (ANR-12-LABXARBRE-01)

We thank Cyril Buré for the help with growing the seedlings and setting up the experiment on the robotic system. Clark and Maxime for their help in harvesting the roots, ONF for harvesting of the seeds, Marie-Beatrice Bogeat-Triboulot for help with the WinRhizo root surface measurements and everyone who helped during the final harvest

Annexe 1 : Means per groups (\pm SE) of Assimilation (A_n), Stomatal conductance (g_s), internal CO_2 concentration (C_i), water use efficiency ($W_i = A_n/g_s$) at each steady-state reached during the measurement cycle (with SS1 the steady-state value at the beginning of the sequence with high light intensity, SS2 the steady-state value obtained at the end of the stomatal closure phase and SS3 the final steady state value when come-back to high). Different letters show the significative differences among groups from the ANOVA model including treatments and species effects tested followed by a post-hoc Tukey test. The significant differences between two steady states from a paired t-test are presented as is (P values: "****" for $P < 0.001$; "***" for $P < 0.01$ and "**" for $P < 0.05$).

STEADY STATE		SS1		SS2		SS3
QPC		10,28 \pm 1,14b	*	8,33 \pm 1,19ab	*	11,07 \pm 0,22a
QPD	A_n - PPFD	6,7 \pm 0,4bc	***	4,59 \pm 0,49bc	***	5,4 \pm 0,87b
QRC	($\mu\text{mol m}^{-2} \text{s}^{-1}$)	14,68 \pm 1,06a	***	11,28 \pm 0,98a	**	14,28 \pm 1,17a
QRD		5,87 \pm 0,6c	**	4,57 \pm 0,6c	***	6,27 \pm 0,83b
	SP	.				**
	T	***		***		***
	SP*T	**				
QPC		0,11 \pm 0,02ab	*	0,08 \pm 0,01ab	ns	0,12 \pm 0,02ab
QPD	g_s - PPFD	0,06 \pm 0,01b	**	0,03 \pm 0b	**	0,04 \pm 0,01b
QRC	($\text{mol m}^{-2} \text{s}^{-1}$)	0,17 \pm 0,03a	***	0,12 \pm 0,02a	**	0,17 \pm 0,02a
QRD		0,05 \pm 0,01b	**	0,04 \pm 0,01b	*	0,06 \pm 0,01b
	SP					*
	T	***		***		***
	SP*T					
QPC		231,62 \pm 16,01a	.	216,31 \pm 11,28a	ns	228,01 \pm 21,17a
QPD	C_i - PPFD	204,04 \pm 19,63a	ns	199,09 \pm 33,08a	ns	192,26 \pm 18,21a
QRC	$\mu\text{mol mol}^{-1}$	233,04 \pm 11,4a	**	211,95 \pm 14,13a	*	233,14 \pm 8,54a
QRD		175,32 \pm 24,27a	ns	169,86 \pm 16,62a	ns	179,41 \pm 19,89a
	SP					
	T	*				*
	SP*T					
QPC		95,1 \pm 10,37a	ns	102,24 \pm 7,07a	ns	94,01 \pm 13,35ab
QPD	W_i - PPFD	121,88 \pm 6,62a	.	135,41 \pm 4,53a	ns	119,34 \pm 10,64ab
QRC	$\mu\text{mol mol}^{-1}$	90,55 \pm 6,39a	*	103,55 \pm 8,72a	*	88,51 \pm 5,3b
QRD		129,78 \pm 15,08a	ns	135,87 \pm 10,96a	ns	128,85 \pm 12,29a
	SP					
	T	**		**		**
	SP*T					

Annexe 2: Photosynthetic parameters for the three A-ci campaigns of measurements (means per groups \pm SE), with the Assimilation (A_{n-Aci}), the Stomatal conductance (g_{s-Aci}), intrinsic water use efficiency ($W_i = A_n/g_s$), the maximum rate of carboxylation (V_{max}) and the maximum rate of electron transport (J_{max}). Different letters show the significative differences among groups from the ANOVA model including treatments and species effects followed by a post-hoc Tukey test. The significant differences between two campaign from a paired t-test are presented as is (P values: “***” for $P < 0.001$; “**” for $P < 0.01$ and “*” for $P < 0.05$).

		F2		F3		F3T
QPC	A_{A-Ci} ($\mu\text{mol m}^{-2} \text{s}^{-1}$)	14,58 \pm 1,14a	ns	12,54 \pm 2,17a	ns	12,07 \pm 1,61a
QPD		16,98 \pm 1,54a	ns	14,53 \pm 0,42a	***	5,62 \pm 0,89b
QRC		13,63 \pm 1,38a	ns	16,42 \pm 1,54a	ns	14,21 \pm 1,34a
QRD		15,23 \pm 2,19a	ns	12,35 \pm 1,79a	*	6,08 \pm 1,05b
	SP					
	T					***
	SP*T					
QPC	g_{A-Ci} ($\text{mol m}^{-2} \text{s}^{-1}$)	0,15 \pm 0,01a	ns	0,11 \pm 0,03a	ns	0,15 \pm 0,03a
QPD		0,2 \pm 0,02a	*	0,12 \pm 0,01a	***	0,05 \pm 0,01b
QRC		0,17 \pm 0,03a	ns	0,2 \pm 0,03a	ns	0,17 \pm 0,02a
QRD		0,19 \pm 0,03a	ns	0,14 \pm 0,02a	**	0,05 \pm 0,01b
	SP			*		
	T					***
	SP*T					
QPC	W_i_{A-Ci} (A/g_s)	98,53 \pm 5,55a	.	123,37 \pm 9,58a	*	89,48 \pm 9,43b
QPD		89,06 \pm 6,89a	*	121,69 \pm 7,62ab	ns	123,78 \pm 7,82a
QRC		88,23 \pm 5,39a	ns	89,3 \pm 6,86c	ns	85,69 \pm 3,3b
QRD		80,97 \pm 3,97a	ns	90,63 \pm 4,88bc	*	133,29 \pm 11,05a
	SP			***		
	T					***
	SP*T					
QPC	V_{max}	47,12 \pm 3,79b	ns	37,19 \pm 7,37b	ns	49,33 \pm 7,03a
QPD		54,07 \pm 5,01b	ns	47,29 \pm 2,96b	ns	41,32 \pm 8,03a
QRC		80,78 \pm 3,98a	.	95,68 \pm 7,57 a	*	64,16 \pm 6,71a
QRD		84,41 \pm 8,53a	ns	78,18 \pm 7,39a	**	36,66 \pm 7,35a
	SP	***		***		
	T					*
	SP*T			*		
QPC	J_{max}	92,45 \pm 11,96b	ns	89,88 \pm 17,98b	ns	85,95 \pm 10,3ab
QPD		118,79 \pm 13,98ab	ns	107,96 \pm 9,09ab	**	53,41 \pm 12,7b
QRC		141,26 \pm 9,74a	ns	168,23 \pm 19,55a	*	114,19 \pm 12,06a
QRD		152,69 \pm 10,46a	ns	119,32 \pm 16,45ab	*	62,46 \pm 13,34b
	SP	***		*		.
	T					**
	SP*T			*		

Annexe 3: Means \pm SE of intrinsic water use efficiency (Wi-m) from pre-selection measurements on 1st and 2nd flushes of oaks seedlings. Lower case letters display groups differences from a two factorial anova model including treatment and species effects (checking for sampling bias).

Groups (n=8/group)	Wi-m	Shapiro-Wilk normality test
QRC	116 \pm 13 ^a	ns
QRD	124 \pm 10 ^a	ns
QPC	100 \pm 11 ^a	ns
QPD	96 \pm 14 ^a	ns

Annexe 4: Ancova table of dynamic parameters, the stomatal anatomy, the water use efficiency estimators and their components (two factorial ancova model including treatment and species effects). The upper-right triangle displays the P-values (with “***” for P<0.001; ”**” for P<0.01 and ”*” for P<0.05), while the lower-left displays the r-values (Pearson test). With the dynamic parameters: τ , λ , SL, their ratio (τ), and the stomatal parameters: GCW (guard cells width), GCL (guard cells length), SS (stomatal size), SD (stomatal density). n=23-32, bold r-values are highly significant (***)

	TE	Bm	TWC	TWCS	BmS	δ13C	Wi PPFD	A _n PPFD	g _s PPFD	Osm	λcl	λop	λr	τcl	τop	τ	SLcl	SLop	SLr	OL	GCL	GCW	SS	SD	
RSD	15.1	31.3	34.5	24.1	20.4	3.9	32.7	50.9	75.8	11.6	64.8	67.4	26.8	51.4	60.4	37.4	54.6	78.0	41.6	5.8	4.9	4.2	8.3	15.6	
TE			**	***		***	*	**	***	***	**	*		**	*										
Bm			***	**	***			*			**	**	*	**	*	*									
TWC	-0.39 (24)	0.90 (54)		***	***	*	*	***	**	**	***	***		***	**										
TWCS	-0.56 (54)	0.35 (54)	0.56 (54)		**	***	*	***	***	*															
BmS		0.56 (54)	0.44 (54)	0.73 (54)				*										*							
δ13C	0.78 (23)		-0.43 (30)	-0.64 (28)			**	***	***	**	***	**		*	**										
Wi	0.51 (24)		-0.45 (26)	-0.48 (26)		0.46 (26)		*	***	*	*														
A _n	-0.59 (24)	0.52 (24)	0.61 (26)	0.70 (26)	0.44 (24)	-0.66 (26)	-0.43 (26)		***	**	***														
PPFD	-0.65 (24)		0.56 (26)	0.68 (26)		-0.69 (26)	-0.65 (26)	0.92 (26)		**	***	**													
g _s PPFD	0.65 (27)		-0.58 (30)	-0.43 (28)		0.52 (30)	0.40 (26)	-0.62 (26)	-0.65 (26)		***	**		**	*										
Osm	-0.74 (22)	0.59 (22)	0.76 (24)	0.43 (22)		-0.68 (24)	0.67 (24)	0.66 (24)	-0.68 (25)		***	**		**	*										
λcl	-0.53 (19)	0.67 (19)	0.71 (21)			-0.63 (21)	0.63 (21)	0.56 (21)	-0.61 (21)	0.90 (19)		***	**	***	***	*									
λop		-0.51 (19)										-0.55 (19)				***									
λr	-0.64 (22)	0.56 (22)	0.69 (24)	0.43 (24)		-0.44 (24)			-0.53 (25)	0.85 (22)	0.80 (19)														
τcl	-0.52 (19)	0.55 (19)	0.57 (21)	0.51 (21)		-0.60 (21)			-0.46 (22)	0.75 (19)	0.86 (19)	-0.5 (19)	0.79 (19)												
τop		-0.46 (19)										-0.44 (19)	0.67 (19)		-0.66 (19)										
τ					-0.44 (22)			-0.53 (24)	-0.55 (24)																
SLcl																									**
SLop																	-0.83 (19)	***		*	*	*	*	*	*
SLr																	0.47 (19)		*	*	*	*	*	*	*
OL																	-0.46 (22)				***	***	***	***	**
GCL																	-0.43 (22)			0.74 (32)		***	***	***	***
GCW																				0.57 (32)	0.72 (32)		***	***	***
SS																				0.71 (32)	0.94 (32)	0.92 (32)		***	*
SD																				-0.44 (22)	0.53 (22)	-0.48 (32)	-0.58 (32)	-0.39 (32)	

Bibliography

- Bacilieri R, Ducouso A, Kremer A (1995) Genetic, morphological, ecological and phenological differentiation between *Quercus petraea* (Matt.) Liebl. and *Quercus robur* L. in a mixed stand of Northwest of France *Silvae Genetica* 44 : 1-9.
- Becker M, Lévy G. (1982) Le dépérissement du chêne en forêt de Tronçais : les causes écologiques. *Ann Sci For* 39:439–444.
- Bréda N, Cochard H, Dreyer E, Granier A (1993) Field comparison of transpiration, stomatal conductance and vulnerability to cavitation of *Quercus petraea* and *Quercus robur* under water stress. *Ann For Sci* 50:571–582.
- Brendel O, Le Thiec D, Saintagne C, Kremer A, Guehl JM (2008) Quantitative trait loci controlling water use efficiency and related traits in *Quercus robur* L. *Tree Genet Genomes* 4:263–278.
- Cernusak L, Winter K, Aranda J, Turner B, Marshall J (2007) Transpiration efficiency of a tropical pioneer tree (*Ficus insipida*) in relation to soil fertility, *J Exp Bot* 58:3549–3566.
- Chevillat VS, Siegwolf RTW, Pepin S, Körner C (2005) Tissue-specific variation of $\delta^{13}\text{C}$ in mature canopy trees in a temperate forest in central Europe. *Bas Appl Ecology* 6:519–534.
- Cochard H, Bréda N, Granier A, Aussenac G (1992) Vulnerability to air embolism of three European oak species (*Quercus petraea* (Matt) Liebl, *Q pubescens* Willd, *Q robur* L). *Ann For Sci* 49:225–233.
- Damour G, Simonneau T, Cochard H, Urban L (2010). An overview of models of stomatal conductance at the leaf level. *Plant Cell Environ* 33:1419–1438
- Dawson TE, Burgess SSO, Tu KP, Oliveira RS, Santiago LS, Fisher JB, Simonin K a, Ambrose AR (2007) Night time transpiration in woody plants from contrasting ecosystems. *Tree Physiology* 27:561–575
- Dickson RE, Tomlinson PT (1996) Oak growth, development and carbon metabolism in response to water stress, *Ann For Sci* 53:81–196.
- Doheny-Adams T, Hunt L, Franks PJ, Beerling DJ, Gray JE (2012) Genetic manipulation of stomatal density influences stomatal size, plant growth and tolerance to restricted water supply across a growth carbon dioxide gradient. *Philos Trans R Soc Lond B Biol Sci.* 367:547–555.
- Dow GJ, Berry JA, Bergmann DC (2014) The physiological importance of developmental mechanisms that enforce proper stomatal spacing in *Arabidopsis thaliana*. *New Phytol* 201:1205–1217.
- Duursma RA, (2015) Plantecophys - An R Package for Analysing and Modelling Leaf Gas Exchange Data. *PLoS ONE* 10, e0143346. doi:10.1371/journal.pone.0143346.
- Epron D, Dreyer (1993) E. Long- term effects of drought on photosynthesis of adult oak trees [*Quercus petraea* (Matt.) Liebl. and *Quercus robur* L.] in a natural stand. *New Phytol* 125:381–389.
- Farquhar GD, Richards RA (1984) Isotopic composition of plant carbon correlates with water-

- use efficiency of wheat genotypes. *Func Plant Biol* 11:539–552.
- Franks PJ, Farquhar GD (2001) The effect of exogenous abscisic acid on stomatal development, stomatal mechanics, and leaf gas exchange in *Tradescantia virginiana*. *Plant Physiol* 125:935–942.
- Franks PJ, Doheny- Adams T, Britton- Harper ZJ, Gray JE (2015) Increasing water- use efficiency directly through genetic manipulation of stomatal density. *New Phytol* 207:188–195.
- Gérardin T, Douthe C, Flexas J, Brendel O. (2018) Shade and drought growth conditions strongly impact dynamic responses of stomata to variations in irradiance in *Nicotiana tabacum*. *Environ Exp Bot* 153:188–197.
- Gieger T, Thomas FM (2002) Effects of defoliation and drought stress on biomass partitioning and water relations of *Quercus robur* and *Quercus petraea*. *Basic Appl Ecol* 3:171–182.
- Gieger T, Thomas FM (2005) Differential response of two Central-European oak species to single and combined stress factors. *Trees* 19:607–618.
- Guehl JM, Picon C, Aussenac G, Gross P (1994) Interactive effects of elevated CO₂ and soil drought on growth and transpiration efficiency and its determinants in two European forest tree species. *Tree Physiol* 14:707–724.
- Günthardt- Goerg MS, Kuster TM, Arend M, Vollenweider P (2013) Foliage response of young central European oaks to air warming, drought and soil type. *Plant Biology* 15:185–197.
- Hu B, Simon J, Rennenberg H (2013) Drought and air warming affect the species-specific levels of stress-related foliar metabolites of three oak species on acidic and calcareous soil, *Tree Physiology*, 33 : 489–504.
- Jones HG (1994) *Plants and Microclimate: A Quantitative Approach to Environmental Plant Physiology*. Cambridge University Press, Cambridge, UK.
- Kaiser E, Morales A, Harbinson J (2018) Fluctuating light takes crop photosynthesis on a rollercoaster ride. *Plant Physiol* 176, 977–989.
- Kardiman R, Ræbild A (2018) Relationship between stomatal density, size and speed of opening in Sumatran rainforest species. *Tree Physiol* 38:696-705
- Kirschbaum MUF, Gross LJ, Percy RW (1988) Observed and modelled stomatal responses to dynamic light environments in the shade plant *Alocasia macrorrhiza*. *Plant Cell Environ* 11:111–121.
- Kleinschmit JRG, Bacilieri R, Kremer A, Roloff A (1995) Comparison of morphological and genetic traits of pedunculate oak (*Q. robur* L.) and sessile oak (*Q. petraea* (Matt.) Liebl.). *Silvae Genetica*, 44:256–269.
- Kuster M, Schleppei P, Hu B, Schulin R, Günthardt-Goerg MS (2013) Nitrogen dynamics in oak model ecosystems subjected to air warming and drought on two different soils. *Plant Biol* 15:220–229.
- Landmann G, Becker M, Delatour C, Dreyer E, Dupouey JL (1993) Oak dieback in France: historical and recent records, possible causes, current investigations. In *Rundgespräche der*

- Kommission für Ökologie Bd 5 (ed. Bayerische Akademie der Wissenschaften), pp. 97-114. Verlag F. Pfeil, Munich.
- Lawson T, Blatt MR (2014) Stomatal size, speed, and responsiveness impact on photosynthesis and water use efficiency. *Plant Physiol* 164:1556–1570.
- Lawson T, von Caemmerer S, Baroli I (2010) Photosynthesis and stomatal behavior. In Lüttge U, Beyschlag W, Büdel B, Francis D (eds) *Progress in botany*, vol 72. Springer, Berlin/Heidelberg, pp 265–304
- Lévy G, Becker M, Duhamel DA (1992) Comparison of the ecology of pedunculate and sessile oaks: radial growth in the Centre and Northwest of France. *For Ecol Manage* 55:51–63.
- Masle J, Gilmore SR, Farquhar G (2005) The ERECTA gene regulates plant transpiration efficiency in *Arabidopsis*. *Nature* 436: 866–870.
- Matthews JS, Vialet-Chabrand SR, Lawson T (2018) Acclimation to fluctuating light impacts the rapidity and diurnal rhythm of stomatal conductance. *Plant Physiol* 176:1939–1951.
- McAusland L, Vialet-Chabrand S, Davey P, Baker NR, Brendel O, Lawson T (2016) Effects of kinetics of light-induced stomatal responses on photosynthesis and water-use efficiency. *New Phytol* 211:1209–1220.
- Nardini A, Tyree, M T (1999) Root and shoot hydraulic conductance of seven *Quercus* species. *Ann For Sci* 56, 371–377.
- Ooba M, Takahashi H (2003) Effect of asymmetric stomatal response on gas-exchange dynamics. *Ecol Modell.* 164:65–82.
- Osonubi O, Davies WJ (1981) Root growth and water relations of oak and birch seedlings. *Oecologia* 51(3) : 343-350.
- Pearcy RW, Schulze ED, Zimmermann R (2000) Measurement of transpiration and leaf conductance. In: Pearcy R.W., Ehleringer J.R., Mooney H.A., Rundel P.W. (eds) *Plant Physiological Ecology*. Springer, Dordrecht pp 137–160.
- Picon C, Guehl J, Aussenac G (1996) Growth dynamics, transpiration and water-use efficiency in *Quercus robur* plants submitted to elevated CO₂ and drought. *Ann For Sci* 53:431–446.
- Pflug EE, Siegwolf R, Buchmann N, Dobbertin M, Kuster TM, Günthardt-Goerg MS, Arend M (2015) Growth cessation uncouples isotopic signals in leaves and tree rings of drought-exposed oak trees. *Tree Physiol* 35:1095–1105.
- Ponton S, Dupouey JL, Bréda N, Feuillat F, Bodénès C, Dreyer E (2001) Carbon isotope discrimination and wood anatomy variations in mixed stands of *Quercus robur* and *Quercus petraea*. *Plant Cell Environ* 24:861–868.
- Ponton S, Dupouey JL, Bréda N, Dreyer E (2002) Comparison of water-use efficiency of seedlings from two sympatric oak species: genotype x environment interactions. *Tree Physiol* 22:413–422.

- Qu M, Hamdani S, Li W, Wang S, Tang J, Chen Z, Song Q, Li M, Zhao H, Chang T (2016) Rapid stomatal response to fluctuating light: an under-explored mechanism to improve drought tolerance in rice. *Funct Plant Biol* 43:727–738.
- Rasheed-Depardieu C, Parelle J, Tatin-Froux F, Parent C, Capelli N (2015) Short-term response to waterlogging in *Quercus petraea* and *Quercus robur*: A study of the root hydraulic responses and the transcriptional pattern of aquaporins. *Plant Physiol Biochem* 97:323–330.
- Roussel M, Le Thiec D, Montpied P, Guehl JM, Brendel O. (2009) Diversity of water use efficiency in a *Quercus robur* family: contribution of related leaf traits. *Ann For Sci* 66:408-417.
- Roussel M, Dreyer E, Montpied P, Le-Provost G, Guehl JM, Brendel O (2008) The diversity of ^{13}C isotope discrimination in a *Quercus robur* full-sib family is associated with differences in intrinsic water use efficiency, transpiration efficiency, and stomatal conductance. *Journal of Experimental Botany* 60 : 2419–2431.
- Sanders TGM, Pitman R, Broadmeadow MSJ (2014) Species-specific climate response of oaks (*Quercus* spp.) under identical environmental conditions. *iforest* 7:61.
- Scotti-Saintagne C, Mariette S, Porth I, Goicoechea P, Barreneche T, Bodénès C, Burg K, Kremer A. (2004) Genome scanning for interspecific differentiation between two closely related oak species [*Quercus robur* L. and *Q. petraea* (Matt.) Liebl.]. *Genetics* 168:1615–1626.
- Shimazaki KI, Doi M, Assmann S, Kinoshita T (2007) Light regulation of stomatal movement. *Annu Rev Plant Biol* 58:219–247.
- Steinbrecher R, Contran N, Gugerli F, Schnitzler JP, Zimmer I, Menard T, Günthardt-Goerg MS (2013) Inter- and intra-specific variability in isoprene production and photosynthesis of Central European oak species. *Plant Biology* 15 :148-156.
- Thomas FM (2000) Growth and water relations of four deciduous tree species (*Fagus sylvatica* L., *Quercus petraea* [Matt.] Liebl., *Q. pubescens* Willd., *Sorbus aria* [L.] Cr.) occurring at central-European tree-line sites on shallow calcareous soils: physiological reactions of seedlings to severe drought, *Flora* 195.
- Thomas FM, Blank R, Hartmann G (2002) Abiotic and biotic factors and their interactions as causes of oak decline in Central Europe. *For Pathol* 32:277–307.
- Thomas FM, Gausling T (2000) Morphological and physiological responses of oak seedlings (*Quercus petraea* and *Q. robur*) to moderate drought. *Ann For Sci* 57:325–333.
- Tyree M, Cochard H (1996) Summer and winter embolism in oak: impact on water relations. *Ann For Sci* 53:173–180.
- Van Hees A (1997) Growth and morphology of pedunculate oak (*Quercus robur* L) and beech (*Fagus sylvatica* L) seedlings in relation to shading and drought. *Ann For Sci* 54:9–18.
- Vialet-Chabrand S, Dreyer E, Brendel O (2013) Performance of a new dynamic model for predicting diurnal time courses of stomatal conductance at the leaf level. *Plant Cell Environ* 36:1529–1546.

- Violet-Chabrand SRM, Matthews JSA, McAusland L, Blatt MR, Griffiths H, Lawson T (2017) Temporal dynamics of stomatal behavior: modeling and implications for photosynthesis and water use. *Plant Physiol* 174:603–613.
- Vico G, Manzoni S, Palmroth S, Katul G (2011) Effects of stomatal delays on the economics of leaf gas exchange under intermittent light regimes. *New Phytol* 192:640–652.
- Wagner P, Dreyer E (1997) Interactive effects of waterlogging and irradiance on the photosynthetic performance of seedlings from three oak species displaying different sensitivities (*Quercus robur*, *Q. petraea* and *Q. rubra*). *Ann For Sci* 54:409–429.
- Welander N, Ottosson B (2000) The influence of low light, drought and fertilization on transpiration and growth in young seedlings of *Quercus robur* L. *For Ecol Manage* 127:139–151.
- Zeppel M, Tissue D, Taylor D, Macinnis-Ng C, Eamus D (2010) Rates of nocturnal transpiration in two evergreen temperate woodland species with differing water-use strategies. *Tree Physiology* 30:988–1000.

Article 3 : Deuxième étude Comparative entre *Q.robur* et *Q.petraea* (H2Oak 2017)

Title: Different Impact of a progressive drought on growth rate and gas exchange between *Quercus robur* and *Quercus petraea*

Authors: Théo Gerardin¹, Oliver Brendel^{1,2}

Adresses:

¹ Université de Lorraine, AgroParisTech, INRA, Silva, F-54000 Nancy, France

³ Corresponding author postal address: Oliver BRENDEL, INRA, UMR Silva, F-542802 CHAMPENOUX, France

Tel : 0033.383394100

ORCID :

Théo P.H. Gerardin: <https://orcid.org/0000-0002-5427-6470>

Oliver Brendel: <https://orcid.org/0000-0003-3252-0273>

Emails: tgerardin.phd@gmail.com, oliver.brendel@inra.fr

Keywords: drought, dynamic response, irradiance, stomatal conductance, growth, oak

Highlights

-Different irradiance closing steps induce similar dynamic responses regardless of the stomatal amplitude

-*Q. petraea* and *Q. robur* seedlings display similar growth and gas exchanges rates under progressive drought although *Q. robur* tended to be sensitive to drought stress earlier.

Abstract

Recent studies have made major progress in describing stomatal dynamics in terms of speed and amplitude of response. Most of past studies described stomatal dynamics as a stomatal conductance variation over a given period of time which is highly dependent of the response amplitude and therefore, the environmental factor inducing stomatal movement. Gas exchange and growth were followed for *Q.petraea* and *Q.robur* during a progressive drought. *Q.robur* had a slightly earlier height growth phenology and was able to maintain diameter growth under medium drought, and even though an earlier stomatal response to progressive drought was observed compared to *Q.petraea*, *robur* was overall able to maintain higher stomatal conductance, assimilation rate, however resulting in a similar intrinsic water use efficiency. Additionally in this study, we measured stomatal dynamics during both opening and closing sequences in response to several different changes in irradiance in two related oaks species (*Quercus robur* and *Quercus petraea*) firstly, under non-limited conditions, then, when oaks seedlings were submitted to an intermediate drought stress. We assessed the temporal response to irradiance changing steps using a dynamic model providing parameters describing the response. Both species displayed similar stomatal behaviours in term of irradiance induced dynamic response, characterized by faster stomatal movements under drought stress and comparable asymmetrical responses regardless of the treatments. Surprisingly two irradiance closing steps of different intensity led to similar kinetics despite divergent stomatal conductance amplitudes induced.

Introduction

Quercus robur and *Quercus petraea* are two sympatric broad-leaved tree species able to hybridize with each other and displaying different ecological behaviours despite a close genetic proximity (Kremer et al., 1993). Adult *Q.robur* trees have been found less resistant to drought episodes than *Q.petraea* (Becker and Levy, 1982; Landmann et al., 1993) and are often distributed on soils with more water as well as nutrient supplies (Levy et al., 1992; Bréda et al., 1993). In addition, higher death rates were reported in *Q.robur* seedlings under severe drought than in *Q.petraea* (Vivin et al., 1993). Soil water deficit is therefore a major environmental constraint to assess. Granier et al., (1999) observed that forest trees including *Q.petraea* experienced a linear loss of canopy transpiration under increasing water stress. Based on these observations Granier et al., (2000) suggested that under 0.4 relative extractible water (REW) most forest trees started experiencing drought stress.

Drought has been found to reduce height and diameter growth in adult *Q.robur* trees stronger and earlier than in *Q.petraea* (Becker 1982; Fonti et al 2013; Friedrich et al., 2008). However, it is less clear under non limited conditions as *Q.robur* has been reported to display higher height growth rates (Ponton et al. 2001,2002; Dobrovolny et al.,2016; Gerard et al., 2009; Parent et al., 2011) and contrasting results were also observed with similar diameter growth rates between the two species (Gieger et al., 2005; Collet et al., 2017) or even higher radial growth in *Q.petraea* (Becker 1986; Lévy et al.,1992). Moreover, Jensen et al. (2000), put in evidence a strong geographical cline for growth in *Q. robur* and *Q.petraea* associated with considerable regional variations that might partly explain the contrasting results observed in literature.

Only a few comparative studies of water use efficiency between the two species have been conducted. In these, *Q.petraea* has been reported with higher intrinsic water use efficiency at the leaf level than *Q.robur* (Epron and Dreyer 1993; Ponton et al., 2001,2002) but contrasting results were also observed, *Q.robur* displaying higher water use efficiency (Thomas et al.,2008) or both species showing no differences (Thomas et al., 2000; Hu et al., 2013). However, the fact that, different water use efficiency estimators were used as well as various experimental designs deployed prevents to draw any firm conclusions about the observed differences. Furthermore, under both control and drought stressed conditions *Q.robur* seedlings were depicted with higher transpiration efficiency than *Q.petraea* Gerardin et al., 2019 (unpublished yet)

Recently, seedlings of the two species from close geographic provenances were reported with comparable stomatal features such as stomatal size and stomatal density, as well as similar stomatal dynamic responses to light under both non-limited and water stressed conditions (Gerardin et al., 2019 (2015).

Response to dynamic light

Irradiance is considered as the main driver of photosynthesis (Shimazaki et al., 2007). Therefore, through the years, steady-state responses to irradiance have been extensively studied. However, such steady-states conditions are unlikely to occur since non-fluctuant conditions are rarely found in nature (Jones, 2013, Vialet-chabrand et al., 2017) as across the day, cloud cover, sun course as well as shading provided by overlapping leaves and neighbouring plants induce numerous fluctuations in irradiance intensity and spectral quality (Way and Pearcy, 2012).

Thus, Incident irradiance on plants leaves is a highly fluctuating environmental factor (i.e. in understory species), causing both dynamic changes in photosynthesis (Kaizer et al., 2018) and stomatal movements (Lawson et al., 2010). The stomatal movements induced by environmental changes translate into temporal processes taking from minutes to hours to reach new steady-states depending on the species (Vico et al., 2011; McAusland et al., 2016) and the magnitude of the irradiance change (Lawson et al 2012; Lawson & Blatt, 2014). The nearly instantaneous photosynthetic response leads to highly uncoupled responses between assimilation and stomatal conductance, which, in turn leads to strong dynamic variations of their balance, known as intrinsic water use efficiency (McAusland et al., 2016). Differences in speed of stomatal movements in response to irradiance has been found among species (Ooba and Takahasi, 2003; Franks and Farquhar, 2007; Drake et al., 2013; Vialet-Charbrand et al., 2013; McAusland et al., 2016) as well as plant functional types (Vico et al., 2011). Moreover, growth conditions impacts were also put in evidence, drier conditions being associated with faster stomatal responses to irradiance (Vico et al., 2011; Qu et al., 2016; Gerardin et al., 2018). However contrasting results were also reported in poplar trees (Durand et al., 2019). Irradiance growth conditions were also associated with altered stomatal responses (Kardminan and Raebild, 2017; Gerardin et al., 2018; Matthews et al., 2018). To describe stomatal behaviour, numerous steady-state models of g_s have been developed (reviewed in Damour et al., 2010) and recently dynamic models have been proposed as reliable alternatives (reviewed in Vialet-Chabrand et al., 2017). Many of the early models initially estimated g_s response to irradiance as a time for g_s to reach another steady state or a given percentage of the global response (Wood and Turner, 1971; Grantz and Zeiger, 1986, Dumont et al., 2013). Another approach was later proposed estimating the rapidity of response by using a regression fit to the linear part of g_s response, hence, providing an estimate of the maximum rate of g_s response (Tinoco-Ojanguren and Pearcy, 1992; Naumburg et al., 2001, Drake et al., 2013). Thus, the temporal response of g_s has been extensively studied in terms of amplitudes and rapidity. However, Vialet-Chabrand et al. (2017) suggested that these approaches could be biased for being too dependent of steady states g_s estimations as well as the linearity of the initial g_s response. Therefore, sigmoidal or exponential dynamic models were proposed (Vialet-chabrand et al., 2013), allowing a fine characterization of both

linear and nonlinear parts of g_s response curves. Several studies have been using such models to characterise the stomatal response to changes in irradiance (McAusland et al., 2016; Gerardin et al., 2018; Gerardin et al., 2019) and VPD (Durand et al., 2019). However, to our knowledge, these publications have not investigated how the different kinetics parameters depends on different applied irradiance step variations. Gerardin et al., (2019) recently showed that for an irradiance step of 400 PPFD, *Q. robur* and *Q. petraea* did not differ in their dynamic of stomatal response under both non-limited and water stressed conditions.

Objectives

The description of *Q. robur* and *Q. petraea* ecology is well documented for adult trees; however, it subsists a gap of knowledge about seedlings and the ecophysiological differences between the two species to fully assess the requirements of their respective ecological niches. In addition, contradictory results were reported. Moreover, providing empirical data about the dynamic stomatal response to irradiance, its asymmetry as well as plasticity to water-stressed conditions might provide new insights to understand the underlying functional and physiological basis involved in drought tolerance and ecology of species.

- i) Characterize the impact of a progressive, controlled drought on growth, gas exchanges and photosynthetic capacity of *Quercus petraea* and *Quercus robur* seedlings
- ii) Study the impact of a medium drought on the dynamic of stomatal response of both species to different step changes in irradiance

Material and methods

Plant material and Experimental design

The experiment was carried out on greenhouse grown *Q. robur* and *Q. petraea* seedlings at the National Institut of Agronomical Research (INRA), Champenoux, France (48°45'8"N, 6°20'28"E, 259m). Acorns used for this experiment were collected in autumn 2015 from mature trees of *Q. robur* and *Q. petraea* originating from 4 pure stands in Northern and North-Eastern France chosen based on water availability gradients in order to represent intra-specific variability. The acorns were initially sown in spring 2016 in 1L pots filled with a mixture of forest soil mixed with pine barks/flax loam and sand 8/2 (v/v), and grown in a shaded common garden. In spring 2017, 12 seedlings originating from 2 different provenances per species were transferred in 6L pots containing a sand, peat and silty-argillaceous forest soil mixture 5/3/2 (v/v/v) inside a greenhouse equipped with a robotic system allowing automatized plant weighting and watering as well as a precise volumetric soil water content (VH for volumetric humidity) monitoring in which they stayed during the whole experiment (for six months from April to August).

Conveyors moved the plants to a weighing and watering station 1-3 times per day during the whole experiment. Each pot was watered to reach an individual target weight calibrated against VH. For each plant, VH was measured regularly on a weekly basis and after a drought level change every day for 3 days. The plant-soil-pot system was weighted directly after VH determination. At the start of the experiment all pots were watered manually to field capacity (~35% of VH). Over the experiment a correlation was established between VH and mass for each pot individually. Allometric correlations based on diameter were used to compensate for plant biomass growth determined previously (Gerardin et al., 2019). The plants were positioned alternatively by species in the greenhouse and first submitted to the same non-limiting growing conditions: natural growth light and well fertilized and irrigated at 70% of the field capacity to avoid water logging until the beginning of the drought. Two *Q. petraea* seedlings died during the greenhouse acclimation period, leaving 12 and 10 plants of *Q. robur* and *Q. petraea*, respectively.

Measurement of soil water status and drought establishment

The volumetric soil water content was measured by time domain reflection (TRIME-TDR; IMKO GmbH, Ettlingen, DE) in each pot at about 10cm depth on a regular basis of 1 measurement per week throughout the experiment to adjust the watering adequately to the aimed drought levels. The air temperature inside the greenhouse followed the environmental variations while never exceeding 25°C due to a cooling system in the facility. The one-year old plants acclimated under well irrigated and

fertilized conditions for 1 months with a soil relative extractable water (REW) >70% and Nitrocote 15g per pot.

The relative extractable water was calculated as $REW = ((HV - Fp) / (Fc - Fp)) * 100$ where HV is the volumetric soil water content, Fp is the HV of wilting point assumed to be at 4% and Fc is the HV at field capacity of each pot/plant .

Then all the plants were progressively submitted to increasing drought levels by stabilising several steps spread over a two months period (from 70% to 25%REW passing by 60-40-35-30% REW levels). The first low REW step was established based on the general drought response threshold detected by Granier (1990) in forest trees species.

-Growth monitoring

The height (H) and the diameter (D) of the plants were measured on a regular basis (every two to three days) throughout the whole experiment. The monitoring started in late April (115th DoY) and finished in mid-July (205th DoY). The height and diameter growth rates (HGR and DGR, respectively) were also calculated from date to date as:

$$HGR = (H_{t+1} - H) / (t_{t+1} - t)$$

$$DGR = (D_{t+1} - D) / (t_{t+1} - t)$$

With H; the height at a given date, H+1 the height at the following date, D; the diameter at a given date, D+1; the diameter at the following date, t; the DoY at a given date, and t+1; DoY at the following date. Additionally, the height and diameter growth rates (HGR' and DGR', respectively) were calculated over the non-stressed period (including the 70 and 60% REW steps over 39 days) as well as over the dry period (including the 40, 35 and 30% REW steps over 37 days) and used in the lower and upper correlations matrix, respectively (Table 3).

Gas exchange monitoring

The gas exchange monitoring was performed using a portable photosynthesis system (LI-COR 6200; LI-COR, Lincoln, NE, USA). Measurements of net CO₂ assimilation rate (A_n), stomatal conductance for water vapour (g_s) were made on a regular basis at each REW level (70-60-40-35-30-25% REW) throughout the whole experiment. For each plant, the measurements were repeated on the same fully sunlit third-flush leaf grown under non-stressed conditions. The monitoring started in late May (143th DoY) and finished in mid-July (198th DoY). Overall 25 measurements were done per plant.

Stomatal dynamics under light change

Two campaigns of measurements were performed on the plants. The first under well irrigated conditions (70%REW level) and the second when plants were submitted to a moderate drought (35% REW level, below the assumed water stressing threshold). Each campaign lasted 1-2weeks and both were spaced from each other by one month. For each plant, all the measurements (well irrigated and drought) were performed on the same third-flush, mature, fully expanded leaf grown under non-stressed conditions.

Dynamic gas exchange was measured using a portable photosynthesis system (LI-COR 6400; LI-COR, Lincoln, NE, USA) equipped with a 2cm² leaf chamber (Li-6400-40). Measured were: net CO₂ assimilation rate (A_n), stomatal conductance for water vapour (g_s). All measurements were carried out between 10:00 and 19:00 h (Central European summer time). The environmental parameters inside the chamber were kept constant during the acclimation phase with [CO₂] entering the chamber of 400 $\mu\text{mol mol}^{-1}$, block temperature of 25°C, air flow of 300 $\mu\text{mol min}^{-1}$ and a PPFD of 1200 $\mu\text{mol m}^{-2} \text{s}^{-1}$ (red/blue irradiance 90/10%, respectively) until the leaf reached a steady-state of g_s . Then a measurement cycle consisted of three step-changes in irradiance reaching another steady state: first A) a single step-change to intermediate irradiance (from 1200 to 400 $\mu\text{mol.m}^{-2} \text{s}^{-1}$ PPFD) inducing a stomatal closure, then B) a single step-change back to the original high irradiance (400 to 1200 $\mu\text{mol.m}^{-2} \text{s}^{-1}$), inducing a stomatal reopening and C) a third single step-change to low irradiance (1200 to 100 $\mu\text{mol.m}^{-2} \text{s}^{-1}$). The stomata were considered in steady-state when g_s did not vary more than $\sim 0.005 \text{ mol m}^{-2} \text{s}^{-1}$ during 10min. Data during the response curves were logged every 60sec. “Steady-state” data as mentioned through the manuscript were calculated for each light level as the mean of 5 points after stabilization of g_s (SD $\sim 0.001 \text{ mol m}^{-2} \text{s}^{-1}$). The obtained response curves were adjusted using the following model.

Dynamic Model description

The stomatal responses of the irradiance curves were adjusted using a sigmoidal model based on Vialet-Chabrand et al., (2013) allowing the estimation of dynamic parameters describing the temporal response of the stomata to an environmental change. The following equation was used:

$$g_s = g_0 + (G - g_0) * \exp(\exp(\lambda - t/\tau))$$

Where g_s is the fitted stomatal conductance, g_0 is the starting value of stomatal conductance (first steady-state obtained after the initial plant acclimation to the environmental conditions inside the Licor chamber right before the irradiance change, g_s sat or g_s low), t is the time, G is the ending value of stomatal conductance (second steady-state reached after the full stomatal response to the irradiance change, g_s sat or g_s low), λ is a time constant describing the lag time of the stomatal response corresponding to the time needed to reach the inflection point of the curve from the moment of the

irradiance change, and τ another time constant describing the response through the steepness of the curve (see Gerardin et al., 2018 for a visual representation of the parameters). From these parameters, the maximum slope (SL) as an estimator of the speed of the stomatal response, has been calculated as: $SL = (1/\tau) * (G - g_0) / \exp$

Where $|(G - g_0)|$ represent the stomatal amplitude of the response (δg_s). Increasing values of τ will affect the curvature of the stomatal response, the smaller a τ value is, the stronger the curvature and the higher SL will be, so the more rapidly g_s will increase/decrease (illustrated in Gerardin et al 2018). The curves were fitted by the model using the function “nlminb” of R (TEAM RC, 2015). The adjustment of the sigmoidal model included five data points during the steady state before changing the irradiance thus delaying the time to reach the inflection of the curves and therefore increasing the values of the lag time λ . These values were then corrected by subtracting the added time period to accurately describe the time needed from the light change. As the model adjustment is sensitive to the starting point values, including five steady state points made the starting steady state g_s more robust and decreases the dependency of the adjustment on measurement noise. The assimilation, conductance and water use efficiency at saturated and low light steady values are mentioned throughout the manuscript as “sat” and “low” respectively.

Additionally, the symmetry of response between the closing (A) and opening (B) sequences has been calculated for each dynamic parameter (τ_r , λ_r and SL_r) as the ratio closing/opening.

A/Ci curves

Similarly to the stomatal kinetic, two campaigns of measurements were performed. First under well irrigated conditions (70%REW level) and the second when plants were submitted to a moderate drought (35% REW level). Gas exchange was measured using a portable photosynthesis system (LI-COR 6400; LI-COR, Lincoln, NE, USA) equipped with a 2cm² leaf chamber. All A-Ci curves were carried out between 09:00 and 18:00 h (Central European summer time). The environmental parameters inside the chamber were kept constant during the acclimation phase at 400 ppm CO₂, with temperature regulated at 25°C, flow at 300 and a photonflux density at 1000 $\mu\text{mol.m}^{-2} \text{s}^{-1}$. All the gas exchange measurements were performed on the same third-flush, mature, fully expanded leaf grown under non-stressed conditions used for kinetics measurements. ([CO₂] sequence: 400-350-300-200-100-0-400-450-600-700-900-1200-1500-1800) “-Aci” suffix added to gaz exchange parameters as mentioned throughout the manuscript refers to the gaz exchange measurements extracted from A-ci curves after the initial step. Aci curves were fitted using the R package “plantecophys” (R core team, 2015) based on the Farquhar-von Caemmerer-Berry model of leaf photosynthesis: FvCB model (Farquhar et al., 1980).

Statistical analysis

All statistical analyses were performed with R (R Core Team (2015)). Effects were analyzed as a two or three factorial design by analysis of variance (ANOVA, Type III error). Significant differences were considered at $P < 0.05$. With the following models used: Table 1,2,3 : Species*Treatment*Lightstep Type III /Table 4,5 : Species*Treatment Type III. The interactions were only shown when found significant

When the ANOVA was found significant, a Post-Hoc test using the Tukey-HSD test (package R, "agricolae") was used to define inter-groups differences. Correlations were estimated using the Pearson method and p-values were adjusted for multiple comparisons using the "p.adjust" function with the false discovery rate method "FDR".

129, then the DGR rapidly increased in both species from 0.04 to 0.28mm.day⁻¹ and 0.02 to 0.22mm.day⁻¹ in QR and QP respectively at day 135(Fig 1d). This coincided with the end of the resting phase for height growth, just before the new flush. Then, both species followed the same growing pattern, the DGR slightly decreased and fluctuated from 0.5 to 1.5mm.day⁻¹ for the rest of the experiment while QR displayed significantly higher DGR between days 166-181.

Gaz exchange monitoring (Fig 2)

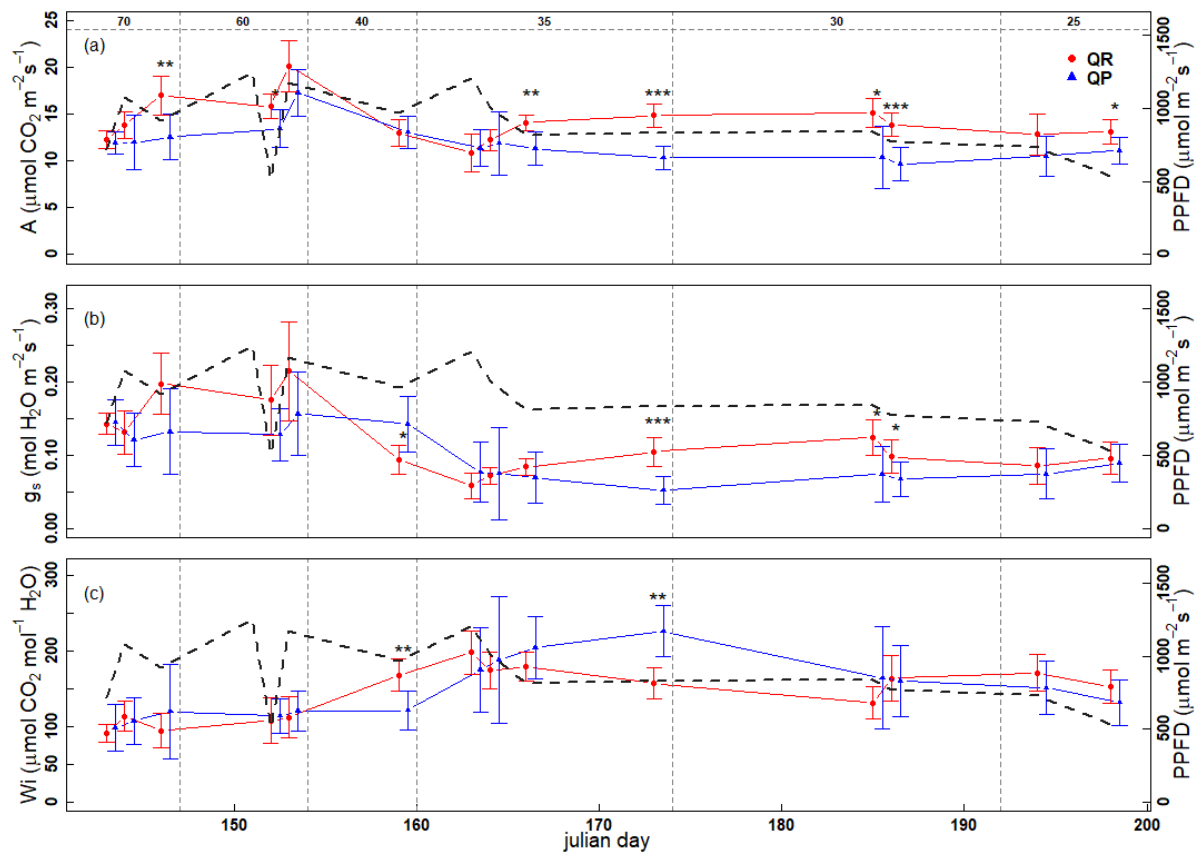


Figure 2 : The monitoring of the net assimilation carbon rate : A (a), the stomatal conductance g_s : (b) and the water use efficiency W_i : (c) through the experiment (mean +- SD). With red dots for QR and blue triangles for QP, the PPFD in black dotted line and the %REW step changes in vertical dotted line. The differences between species at given date from a t-test are presented as : P values : “****” for $P < 0.001$; “***” for $P < 0.01$ and “**” for $P < 0.05$. To avoid overlapping values and improve the visibility, QP monitoring has been shifted by a day. See Annexe 1 for Tuckey-HSD results.

At the beginning of the experiment when the plants were submitted to non-stressed conditions (% REW 70 and 60), both species displayed similar A_n values $\sim 12.0 \mu\text{molm}^{-2}\text{s}^{-1}$. Then, A_n slightly increased in both species QR displaying significantly higher values than QP at days 144 and 152. After that, A_n decreased again to similar values $\sim 13.0 \mu\text{molm}^{-2}\text{s}^{-1}$ in both species for the 40%rew step and $\sim 11 \mu\text{molm}^{-2}\text{s}^{-1}$ at the beginning of the 35%rew step. The assimilation rate remained at this level for the rest of the

experiment for QP, while it slightly re-increased and stabilized in QR resulting in significantly higher A_n values $\sim 14 \mu\text{mol m}^{-2}\text{s}^{-1}$ till the experiment end at day 198 (Fig 2a).

The stomatal conductance g_s followed a similar starting pattern, both species displaying similar values under non-stressed conditions, then g_s dropped significantly in QR during the 40% REW step while it remained constant in QP (Fig 2b). For QP the g_s values started to drop at the first measurement during the 35% REW level, reaching similar values as QP. Then the stomatal conductance remained relatively constant till the end of the experiment in QP while it re-increased similarly to A_n in QR, resulting in significantly higher g_s between days 173-186.

The similar A_n and g_s values resulted in similar $W_i \sim 110 \mu\text{mol mol}^{-1}$ in both species under non-stressed conditions (Fig 2c). Then W_i increased to $\sim 168 \mu\text{mol mol}^{-1}$ concomitantly to the g_s drop in QR at the 40% REW step while it remains stable in QP. The W_i continued to increase in QR at the beginning of 35%rew step and fluctuated around a relatively constant level for the rest of the experiment While W_i values in QP started to increase at the beginning and reached their highest values at the end of the of the 35% REW step concomitantly to the lowest g_s values resulting in significantly higher W_i in QP than QR. Then QP W_i values slightly decreased to similar values than QR until the end of the monitoring (Fig 2c). See annexe I for the Tuckey-HSD table by days and species.

Dynamic response to irradiance

Both oak species displayed similar dynamic response for all three parameters (τ , λ and SL) during both wet and drought campaigns (Table 1). The responses were significantly faster under drought for all three parameters sequences (lower values for τ and λ and higher SL values). Additionally, in the two campaigns, τ and λ of both closing sequences (A and C) were not significantly different whereas SL values showed a significant difference between A and C sequences. All three parameters were significantly different between the closing and opening sequences of the same irradiance step (A and B, respectively) with slower stomatal movements during opening. This can be seen in the τ_r and λ_r values, which were inferior to 1, whereas values of SL_r were superior to 1. This asymmetry was not significantly affected by the drought treatment.

Table 1 : Dynamic parameters from the two campaigns of irradiance response curves (means +SE), with tau the response time, L : the lag time and SL ; the maximal slope. With uppercase letters referring to the light step (see Fig 1) and the lower case letters presenting the results of Post-hoc Tukey test when STEP effect was found significant. As no interactions between factors were found interactions lines do not figure in the table. ($n = 10-12$ observations per group and Anova P values: “****” for $P < 0.001$; ”***” for $P < 0.01$, ”**” for $P < 0.05$ and for $0.05 > P > 0.1$, “.”)

species	step			Wet	Drought
QP	A	1		287 ± 57ab	86 ± 7bc
QR	A			159 ± 29abc	86 ± 9c
QP	B	2	τ	359 ± 102a	126 ± 21abc
QR	B		(sec)	320 ± 103a	168 ± 22abc
QP	C	1		176 ± 29abc	63 ± 6c
QR	C			143 ± 28abc	78 ± 8c
SP	.				
STEP	***				
TTMT	***				
SP*T	.				
QP	A	1		243 ± 40abc	121 ± 22c
QR	A			231 ± 23bc	163 ± 15c
QP	B	2	λ	425 ± 132ab	203 ± 19bc
QR	B		(sec)	435 ± 90a	210 ± 22bc
QP	C	1		202 ± 29bc	129 ± 11c
QR	C			225 ± 25bc	148 ± 14c
SP	.				
STEP	***				
TTMT	***				
SP*T	.				
QP	A	2		1.15 ± 0.38b	1.59 ± 0.36ab
QR	A			2.04 ± 0.4ab	1.67 ± 0.21ab
QP	B	1	SL	0.88 ± 0.36b	1.43 ± 0.46ab
QR	B		(m ⁻² s ⁻²)	1.00 ± 0.25b	0.89 ± 0.17b
QP	C	3		2.35 ± 0.64ab	3.24 ± 0.58a
QR	C			3.3 ± 0.7a	3 ± 0.31a
SP	.				
STEP	***				
T	.				

Steady state measurements and amplitudes of response

Both species displayed similar g_s values at saturating light steady-states from each light change curves $\sim 0.11 \text{ mol m}^{-2} \text{ s}^{-1}$, overall g_s decreased significantly under drought conditions. At low light steady state, no difference between species was observable g_s stabilized at ~ 0.067 for A and B sequences during the control while it stabilized at significantly lower values for C ~ 0.03 . The same pattern between A, B and C was observable during the drought campaign (Table 2).

The absolute amplitude of stomatal response δg_s was significantly reduced under drought conditions for all three sequences. In additions, δg_s was significantly higher during the C sequence than the two others. The same variations were observable in Δg_s with the highest relative amplitude in C $\sim 70\%$, but the responses were similar during both campaigns (Table 2).

A_n followed a similar trend to g_s during the wet campaign, at saturating light there was still no difference between light sequences but this time QR displayed significantly higher values than QP. Similarly to g_s , the assimilation values were significantly reduced under drought conditions, QR still displaying higher rates than QP. At low light steady states, A and B had similar values slightly higher in QR and similarly to g_s , the lowest A_n were obtain after the C sequence, reaching ~ 2.4 and $\sim 2.1 \mu\text{mol m}^{-2} \text{ s}^{-1}$ under wet and drought conditions respectively. The differences between the Wet and drought campaigns were still significant, wet reduced at low light steady state (Table 2).

The absolute and relative amplitude of response of assimilation, δA_n and ΔA_n , respectively, followed the same pattern than δg_s and Δg_s , the highest amplitude of response being observed in the C sequences $\sim 80\%$, δA_n being reduced under drought and both campaigns displaying similar ΔA_n (Table 3).

Regarding W_i both species displayed similar values at high steady state during both campaign, W_i being significantly higher under drought conditions. At low light steady state there was still no differences between species and W_i values were still slightly higher under drought conditions, however this time W_i was significantly lower in C than the two other sequences during both campaigns following the higher ΔA_n than Δg_s (Table 3).

Table 2 : Steady state gaz exchange measurements from each campaign (means + SE), with A_n the CO₂ net assimilation rate, g_s the stomatal conductance and W_i the intrinsic water use efficiency at saturating light (-sat) and low light (-low). uppercase letters refer to the light step and the lower case letters present the results of a Post-hoc Tuckey test. ($n = 10-12$ observations per group and P values: “***” for $P < 0.001$; ”**” for $P < 0.01$, ”*” for $P < 0.05$ and , “. ” for $0.05 > P > 0.1$).

		Wet	Drought			Wet	Drought
QP	A	0.1 ± 0.01a	0.08 ± 0.01a	QP	A	0.053 ± 0.01abc	0.047 ± 0.01abcd
QR	A	0.13 ± 0.02a	0.09 ± 0.01a	QR	A	0.069 ± 0.01a	0.049 ± 0abcd
QP	B	g_s -sat 0.11 ± 0.02a	0.09 ± 0.01a	QP	B	g_s -low 0.066 ± 0.01ab	0.050 ± 0.01abcd
QR	B	0.12 ± 0.01a	0.09 ± 0.01a	QR	B	0.069 ± 0.01a	0.051 ± 0abc
QP	C	0.11 ± 0.02a	0.07 ± 0.01a	QP	C	0.031 ± 0bcd	0.021 ± 0d
QR	C	0.12 ± 0.01a	0.08 ± 0.01a	QR	C	0.027 ± 0cd	0.023 ± 0cd
SP		.	.	SP		.	.
STEP		.	.	STEP	***	.	.
TTMT	***	.	.	TTMT	***	.	.
QP	A	10.7 ± 0.82ab	9.48 ± 1.14ab	QP	A	5.92 ± 0.91a	6.18 ± 0.88a
QR	A	13.32 ± 0.84a	10.5 ± 0.69ab	QR	A	8.04 ± 0.85a	6.73 ± 0.46a
QP	B	A_n -sat 10.72 ± 0.87ab	9.87 ± 1.12ab	QP	B	A_n -low 7.42 ± 0.79a	6.68 ± 0.86a
QR	B	12.62 ± 0.72ab	10.28 ± 0.8ab	QR	B	8.31 ± 0.48a	6.76 ± 0.5a
QP	C	11.31 ± 0.93ab	8.5 ± 0.69b	QP	C	2.44 ± 0.31b	2.09 ± 0.32b
QR	C	12.49 ± 0.73ab	10.12 ± 0.74ab	QR	C	2.35 ± 0.2b	2.16 ± 0.27b
SP	**	.	.	SP	*	.	.
STEP		.	.	STEP	***	.	.
TTMT	***	.	.	TTMT	*	.	.
QP	A	111.66 ± 7.98a	125.19 ± 6.52a	QP	A	117.89 ± 7.13abc	131.11 ± 6.2ab
QR	A	110.24 ± 8.25a	128.24 ± 7.2a	QR	A	124.66 ± 6.25ab	140.63 ± 6.95a
QP	B	W_i -sat 108.58 ± 12.95a	116.57 ± 5.38a	QP	B	W_i -low 119.74 ± 9.69abc	131.09 ± 6.45ab
QR	B	115.89 ± 8.45a	123.63 ± 6.81a	QR	B	126.06 ± 6.24ab	135.45 ± 6.51a
QP	C	111.51 ± 11.26a	121.59 ± 4.56a	QP	C	79.51 ± 3.99d	99.03 ± 12.3bcd
QR	C	110.59 ± 9.23a	126.48 ± 8a	QR	C	88.7 ± 5.9cd	91.97 ± 7.44cd
SP		.	.	SP		.	.
STEP		.	.	STEP	***	.	.
TTMT	**	.	.	TTMT	*	.	.

Table 3 : Amplitudes of responses to irradiance changes (mean +SE) with δ and Δ the absolute and relative amplitudes, respectively). uppercase letters refer to the light step and the lower case letters present the results of a Post-hoc Tuckey test. ($n = 10-12$ observations per group and P values: “***” for $P < 0.001$; ”**” for $P < 0.01$, ”*” for $P < 0.05$ and for $0.05 > P < 0.1$, “.”).

species	step		Wet	Drought
QP	A		4,78 ± 0,66cd	3,3 ± 0,37d
QR	A		5,27 ± 0,44cd	3,78 ± 0,32d
QP	B	δAn	3,3 ± 0,43d	3,19 ± 0,45d
QR	B		4,31 ± 0,42cd	3,52 ± 0,48d
QP	C		8,87 ± 0,76ab	6,75 ± 0,97bc
QR	C		10,14 ± 0,72a	7,96 ± 0,71ab
SP	.			
STEP	***			
T	***			
QP	A		-46 ± 6,01a	-36,14 ± 3,44a
QR	A		-41,11 ± 4,17a	-35,8 ± 1,76a
QP	B	ΔAn	-31,22 ± 4,44a	-33,17 ± 3,87a
QR	B		-33,91 ± 2,53a	-32,94 ± 3,04a
QP	C		-78,55 ± 2,03b	-76,07 ± 2,3b
QR	C		-80,73 ± 1,84b	-77,94 ± 2,49b
SP	.			
STEP	***			
T	***			
QP	A		0,05 ± 0,01bc	0,03 ± 0,01c
QR	A		0,06 ± 0,01abc	0,04 ± 0,01c
QP	B	δg_s	0,05 ± 0,01bc	0,04 ± 0,01bc
QR	B		0,05 ± 0,01bc	0,03 ± 0,01c
QP	C		0,08 ± 0,01ab	0,06 ± 0,01abc
QR	C		0,09 ± 0,01a	0,06 ± 0,01abc
SP	.			
STEP	***			
T	***			
QP	A		-50,63 ± 4,47a	-39,68 ± 1,86a
QR	A		-49,24 ± 3,48a	-41,08 ± 2,89a
QP	B		-38,65 ± 5,26a	-40,98 ± 2,18a
QR	B	Δg_s	-39,83 ± 3,04a	-38,57 ± 3,58a
QP	C		-71,1 ± 2,11b	-67,96 ± 3,94b
QR	C		-76,12 ± 2,58b	-71 ± 2,04b
SP	.			
STEP	***			
T	*			

Photosynthetic capacity

The photosynthetic capacity was significantly reduced under drought in both species, V_{max} and J_{max} displaying lower values than under control condition, moreover QR displayed significantly higher V_{max} values than QP especially under control conditions. Thus, overall QR displayed higher A_n rates associated with a better photosynthetic capacity.

Table 4 : Photosynthetic capacity values from Aci curves. Different letters show the significative differences between groups from a two factors ANOVA model including treatment and species effects followed by a post-hoc Tukey test. ($n = 22$ observations per group and P values: “****” for $P < 0.001$; “***” for $P < 0.01$ and “**” for $P < 0.05$).

species	Parameter	Control	Drought
QP	V_{max}	$51,5 \pm 5,5ab$	$42,2 \pm 5,4b$
QR		$72,4 \pm 7,5a$	$51,9 \pm 5,0ab$
SP	*		
T	*		
SP*T			
QP	J_{max}	$82,1 \pm 14,4ab$	$55,4 \pm 7,0b$
QR		$105,8 \pm 8,1a$	$67,8 \pm 6,7b$
SP	.		
T	***		
SP*T			

Correlation matrix

Intrinsic water use efficiency is calculated as the ratio between assimilation rate and stomatal conductance. These two components are linked by a nonlinear relationship and known to influence each other variations (i.e stomatal limitation other A_n). The present results suggested that W_i variations among treatments for both light saturated as well as field measurements were mainly driven by g_s .(Table 5)

Although we found highly different dynamics between irradiance steps, especially between the opening the sequence and the two others, regardless of the treatments, our results have shown a globally coordinated dynamic response between the different irradiance steps under control conditions since all parameters displayed relatively high correlations between each others. Under drought, the stress seemed to disrupt the previous coordination as most of the correlations disappeared. Nevertheless, correlations between same parameters were still observable (exception made of τ_c/τ_b and λ_a/λ_b) thus indicating the maintenance of common mechanisms involved in the response to several irradiance steps under drought stress.

Interestingly, the asymmetry of response between closing and opening was systematically driven by variations in the opening sequences parameters (as shown by the negative correlations found for τ_r/τ_b , λ_r/λ_b and SL_r/SL_b) in both treatments.

In addition, all dynamic parameters extracted from the first irradiance step (A) appeared to correlate negatively (τ and λ) and positively (SL) to the photosynthetic capacity (equivalent correlations for V_{max} and J_{max} which themselves correlated with each other). Interestingly field measurements Intrinsic water efficiency were negatively correlated with photosynthetic capacity as well as positively with dynamics parameters.

Surprisingly, when found significant, we observed the opposite relationships between W_i and dynamic parameters under water stressed conditions (negative correlations for λ_a/W_i , λ_b/W_i and positive for SL_b/W_i , SL_c/W_i). Additionally, irradiance curves were performed at different period of the throughout the experiment. Therefore, we tested a potential hour of measurements effect on dynamic parameters and g_s steady state values. No effect was detected on any of the parameters (ANOVA $P > 0.05$; data unshown).

Table 5 : Correlation matrix between the dynamic parameters (τ, λ, SL), their closing/opening ratios (τ_r, λ_r, SL_r), the photosynthetic parameters (V_{max} and J_{max}), gas exchange monitoring measurements (A_n-m, g_s-m, W_i-m) and the growth rates (DGR' and HGR') under control conditions (lower matrix) et drought condition (upper matrix). R-value, P-value and number of observations are presented for each parameters with P values : “***” for $P < 0.001$; “**” for $P < 0.01$ and “*” for $P < 0.05$.

	λ_a	λ_b	λ_c	λ_a	λ_b	λ_c	SLa	SLb	SLc	λ_r	λ_r	SLr	A_n-m	g_s-m	W_i-m	V_{max}	J_{max}	DRG	HRG	
λ_a		0,62**(20)	0,49*(21)				-0,53*(21)		-0,49*(21)											
λ_b	0,87***(17)					0,66**(20)		-0,53*(20)	-0,5*(20)	-0,63**(20)	-0,45*(20)	0,66**(20)								
λ_c	0,82***(18)	0,74**(16)												0,69***(20)	-0,66**(19)					
λ_a	0,84***(22)	0,69**(17)	0,76***(18)			0,76***(21)					0,5*(20)									-0,48*(19)
λ_b	0,85***(17)	0,94***(17)	0,69**(16)	0,76***(17)		0,47*(20)					0,57**(20)	0,46*(20)								
λ_c	0,67**(18)	0,69**(16)	0,84***(18)	0,88***(18)	0,74**(16)															
SLa	0,74***(22)	-0,62**(17)	-0,65**(18)	-0,65**(22)	0,65**(17)	-0,54*(18)		0,81***(20)	0,83***(21)											
SLb	-0,72**(17)	-0,63**(17)	-0,67**(16)	-0,72**(17)	0,66**(17)	-0,7*(16)	0,92***(17)		0,79***(20)				0,57**(20)							0,47*(19)
SLc	-0,7**(18)	-0,66**(16)	0,78***(18)	0,72***(18)	0,67**(16)	-0,65**(18)	0,91***(18)	0,9***(16)					-0,47*(20)							0,57**(21)
λ_r		-0,51*(17)			-0,51*(17)															
λ_r		-0,59*(17)			0,66**(17)					0,75***(17)										
SLr	0,63**(17)			0,69**(17)				-0,56*(17)												
A_n-m															0,71***(20)					0,51*(19)
g_s-m														0,64***(22)		0,86***(19)				
W_i-m	0,6**(22)			0,58**(22)			-0,46*(22)	-0,5*(17)	-0,48*(18)				-0,52*(22)	0,89***(22)						
V_{max}	-0,68**(18)			-0,58*(18)	-0,54*(14)		0,52*(18)						0,56*(18)		-0,58*(18)					0,58**(20)
J_{max}	-0,66**(20)			-0,55*(20)	-0,57*(16)		0,53*(20)							0,52*(20)	-0,61**(20)	0,69**(18)				
DRG																				
HRG																				0,54*(22)

Table 6: Correlation matrix between the steady states values (A_n , g_s , W_i), gaz exchange monitoring efficiencies (W_i -m and W_{inst} -m) and growth rates (DGR' and HGR') under control conditions (lower matrix) et drought condition (upper matrix). R-value, P-value and number of observations are presented for each parameters with P values : “***” for $P < 0.001$; “**” for $P < 0.01$ and “*” for $P < 0.05$.

	g_s sat	g_s low	A_n sat	A_n low	W_i sat	W_i low	W_i -m	W_{inst} -m	DGR'	HGR'
g_s sat		0,93 *** 21	0,87 *** 21	0,88 *** 21	-0,70 *** 21				0,48 * 21	
g_s low	0,92 *** 22		0,81 *** 21	0,89 *** 21	-0,68 *** 21	-0,44 * 21			0,51 * 21	
A_n sat	0,73 *** 22								0,44 * 21	0,44 * 21
A_n low	0,80 *** 22		0,83 *** 22						0,49 * 21	
W_i sat	-0,86 *** 22	-0,76 *** 22		-11,66		0,71 *** 21				
W_i low	-0,67 *** 22	-0,61 ** 22			0,84 *** 22		0,58 ** 20	0,62 ** 20		
W_i -m	-11,22		-10,56	-10,78	0,54 ** 22			0,96 *** 20		
W_{inst} -m	-11,22		-12,54	-10,78	0,55 ** 22		0,98 *** 22			
DGR'										
HGR'									0,53 * 22	

Discussion

Drought impact on growth

We monitored the growing patterns of oaks seedlings during their second season of vegetation marked by a progressive drought. Both species displayed highly similar growth patterns for both height and diameter across the experiment although *Q. robur* displayed higher initial heights and diameters as well as a few episodes of higher growth rates. These observations match previous works on the same species (Levy et al., 1992) and might partly explained the pioneer behavior often reported for *Q. robur*. Interestingly, the two species seemed to alternate Height and diameter maximal growing periods, the establishment of the 3rd flush matching with the height growth peak around the 150th DoY. Nevertheless, such pattern was suggested in a previous study on oaks seedlings (Payan, 1982) and alternate growing patterns between height and roots biomass were also reported inside the *Quercus* family (Willaume & Pagès, 2011). Moreover, plants diameter kept growing until the end of the monitoring at more erratic rates. Such behaviors might suggest a strategy of acclimation to drought by breaking the rhythmic growth patterns and switching the available structural carbon allocation into others compartments such as storage organs. Thus, avoiding the emergence of new flushes and by extension more transpiring surface.

Furthermore, In the present study we did not established any relationship between diameter and height growth rates and the others recorded parameters over the well irrigated period. However, during drought, we established a link between gaz exchanges at both saturating and low light steady states and the diameter growth rate. It is worth noticing that these correlations with diameter growth were slightly higher than for the stomatal conductance than assimilation rates and yet very close which might indicate a stomatal limitation over CO₂ assimilation driving the diameter growth rate. However, the apparent rhythmic growth rates in oak during flushes establishment and therefore a nonlinear growth may complexify any interpretations, especially since a flush-establishment period overlapped both non stressed and droughted conditions.

Drought response impact on gas exchanges

In order to characterize the drought response of the two oaks species, we performed two campaigns of measurements before and during drought stress (at 70 et 40% REW, respectively) from which we extracted steady states data. Additionally, we monitored gaz exchanges on a weekly basis during the whole experiment. Gaz exchange whether extracted from steady states measurements (Aci and irradiance response curves) or from the monitoring tended to converge to the same conclusions despite a few discordancy. Overall, both species displayed equivalent responses to drought by decreasing g_s and A_n while increasing W_i and the only difference between species was higher

assimilation rates in *Q. robur* associated with better photosynthetic capacity regardless of the water status. However, as indicated in the introduction, the few comparative publications available in the literature display numerous conflicting results about differences between the two species in W_i . Thus in some studies both species displayed similar W_i levels (Scuiller 1990 ; Vivin et al., 1993 ; Thomas & Gausling 2000) while others suggested higher W_i in *Q. petraea* than *Q. robur* mostly attributed to differences in stomatal conductance (Epron & Dreyer, 1993 ; Ponton et al., 2001 ; Roussel et al., 2009a). Overall, interspecific differences tends to be consistent in adults trees, *Q. petraea* displaying a higher W_i while reports on seedlings seems more conflicting. In accordance with our steady states measurements, during most of the monitoring *Q. robur* showed higher assimilation rates than *Q. petraea* as well as stomatal conductance and despite two antagonistic W_i measurements, both species followed globally the same trend over the progressive drought, reaching what seemed to be their maximal plasticity to drought under 35%rew. Nevertheless, it is worth noticing that during the transition from 60%rew to 40% the stomatal conductance of *Q. robur* dropped leading to significantly higher W_i than *Q. petraea* whose stomatal conductance dropped at lower REW during the 40-35%rew transition. Such results might indicate the existence of different drought triggering thresholds between the two species but in order to either comfort or disregard this thesis another experiment including more repetitions as well as a more refine design of REW steps would be required. Furthermore, one must take into account that both gaz exchange methods used in the present study carry their own restrictions. Steady states measurements although being recorded under controlled conditions are unlikely to occur in nature as plants are submitted to a highly fluctuant environment and might therefore, provide a biased view of gaz exchanges far from the actual field conditions. On the other hand, field monitoring is prone to less accurate gaz exchange estimations which is susceptible to hide fine variations in CO_2 uptake as well as stomatal conductance. Therefore we will remain careful by concluding that both species displayed similar responses to drought as well as W_i levels and that the differences in assimilation rates are likely to be involved in the better growth observed in *Q. robur* seedlings providing a strong competitive advantage.

Stomatal dynamics

Acclimation to drought

Along with gas exchange measurements, two campaigns of irradiance response curves were performed in order to assess drought impact on stomatal dynamics as well as differences in dynamics between irradiance steps of different magnitudes. Kirschbaum et al. (1988) proposed a dynamic model in which the response to irradiance was hypothesized to be composed of three functional steps: first, a biochemical signal that responds directly to irradiance, then a subsequent variation of osmotic potential and a final water transportation in/out guard cells, inducing the actual stomatal movement.

We applied a dynamic model on the obtained sigmoidal responses to irradiance from which we extracted two parameters expressed as time constants independent of stomatal amplitudes and describing the shape of the response curves. λ was defined as a lag time estimate related to the first biochemical signal response induced by the irradiance change while τ described the steepness of the sigmoid curve likely linked to ion and water fluxes operating during stomatal movements (Blatt, 2000). The third dynamic parameter provided by the model was a maximal stomatal response slope estimate (SL) dependent of the actual amplitude of g_s .

Both species displayed matching dynamic responses regardless of the treatments or, the irradiance steps (A, B, C) for all three dynamic parameters. These results are consistent with our previous study on the same species in which *Q. robur* and *Q. petraea* exhibited the same stomatal behavior characterized by faster responses under drought stress (Gerardin et al., 2019) and is comforted by the few other studies assessing stomatal dynamics under water stress also highlighting faster responses in drier climate (Vico et al., 2011) and experimental drought (Qu et al., 2016 ; Haworth et al., 2018). It is also worth mentioning that other factors were also reported to impact stomatal dynamics such as irradiance growth levels (Kardiman and Raebild, 2017 ; Matthews et al., 2018 ; Gerardin et al., 2018), stomatal features (Franks and Farquhar, 2007 ; Drake et al., 2013 ; Raven 2014 ; Aasama and Aphalo, 2016 ; Xiong et al., 2017) or stomata functional type (McAusland et al., 2016). Most of the studies assessing the relationship between stomatal morphology and dynamics reported faster responses associated with smaller stomata as well as higher stomatal density. Nevertheless, in Gerardin et al., (2019) seedlings of the same age from the same species displayed analogous stomatal features under both non limited and experimental drought conditions. Furthermore, no relationship between dynamic parameters and stomatal traits were established. Thus, we assumed in the present study that stomatal morphology did not play any significant role in the observed dynamics variability.

Symmetry of dynamic parameters

Very few studies explored the symmetry of response between stomatal closing and opening. Ooba and Takahashi (2003) found that most species from irradiance-limited environment displayed mostly asymmetrical responses marked by faster opening than closing. Such behaviour has been suggested to help overcome the stomatal limitation that constrain CO_2 diffusion during stomatal opening and therefore, improve CO_2 net assimilation (Lawson et al., 2010, 2012; Violet-Chabrand et al., 2013; McAusland et al., 2016). However, Ooba & Takahashi (2003) also suggested through modelling that the asymmetry controls water use by transpiration rates rather than carbon gain under fluctuating irradiance. In previous studies, we found conflicting results about drought impact on the symmetry of stomatal response to irradiance. In tobacco plants submitted to water stress conditions, the

asymmetry decreased compared to control plants due to relatively faster opening (Gerardin et al., 2018). Despite such differences in drought acclimation among species, the previous study that we conducted on *Quercus robur* and *Quercus petraea* seedlings (Gerardin et al., 2019) is consistent with the results of the present work, both experiment revealing slower opening responses than closing, no modifications of the symmetry under drought stress and comparable symmetry values between the two species. Such consistent results tend to suggest that even if dynamic response asymmetry plays a role in CO₂ uptake or water loss it doesn't seem to take a part in the acclimation process to drought in young oaks seedlings neither in the differentiation of their respective ecological niche.

Comparison of irradiance steps

First of all, the matching closing and opening sequences (A and B) displayed the same amplitudes of stomatal conductance as well as assimilation rates in both absolute and relative terms (~45% stomatal reduction compared to the saturating steady states). Furthermore, as expected the closing sequence induced by a more intense irradiance step (C) resulted in a stomatal closure of a larger extent (~70%).

Interestingly, the three dynamic parameters followed the same trend when plants were submitted to a drought stress and although the δg_s and δA_n were reduced due to the stress and their relative responses remained slightly unchanged. Such results might indicate that despite numerous physiological functions impaired under drought such as photosynthetic capacity some processes involved in the response to irradiance remain fully operational.

As hinted by the depiction of the symmetry, differences between irradiance steps dynamics were found. Regardless of the treatment, opening sequences (B) were systematically slower for all three parameters than their counter part closing sequences induced by the same antagonistic irradiance step (A), but also the second closing sequence (C). Nevertheless, while we may have expected well differentiated dynamics associated with each irradiance steps. For both closing sequences (A and C), relative and absolute amplitudes (g_s and A_n) were significantly different, resulting also in a difference in maximal slope (SL), whereas the time constants (λ and τ) were not affected by the magnitude of the irradiance step. These results may imply that some of the mechanisms involved in the response to irradiance are not proportional to the intensity of the stimuli but rather its nature or are unrelated and dependant of completely different factors such as plant intrinsic properties. Obviously, such assumption would require further experiments including a wider range of irradiance steps tested for both stomatal opening and closing.

Such findings highlight the importance of decomposing the temporal response into parameters describing specific aspects of the dynamics, otherwise interesting differences or in our case similarities

would remain unveiled if a more direct approach had been employed. Moreover, our results hinted the coexistence of plastic and invariant process involved in the dynamic response to irradiance

Conclusion

In this study, we highlighted the impact of drought on the dynamic response of stomata to several step variations in irradiance in *Q.petraea* and *Q.robur* seedlings. Drought treatment led to faster dynamics in both species. The similar dynamics displayed by the two species tends to suggest that in oak the temporal response to irradiance might not be involved in the differentiation of their respective ecological requirements. However, such assertion needs to be confirmed in a bigger extent in the near future. Additionally, the progressive drought reached an extent at which vertical growth was altered and diameter growth strongly reduced in both species. Gas exchanges were also significantly reduced leading to an increase of water use efficiency. Nevertheless, *Q.robur* seemed to be more sensitive to the progressive drought by displaying these changes at a higher water availability than *Q.petraea*, thus hinting toward species specific drought-response threshold. Such result might have considerable implications in regard of their respective ecological niches. An important perspective would be to confirm the coherence of these results with further progressive drought experiments.

Declaration of interest

All authors disclose any financial or personal conflict of interest.

Author contributions

OB and TG designed the experiment, OB provided study material and environment, TG, and OB conducted the experiment, TG, OB did the data analysis, and TG, OB wrote the manuscript and were involved in the interpretation and critical discussion of the results, OB obtained funding.

Acknowledgements

TG acknowledges the PhD grant from the H2Oak ANR-14-CE02-0013 project. This study was part of the interdisciplinary « H2Oak » research project aiming to investigate the diversity for adaptive traits related to water use in two European white oaks (*Quercus robur* and *Quercus petraea*). The UMR Silva is supported by the French National Research Agency through the Laboratory of Excellence ARBRE (ANR-12-LABXARBRE-01)

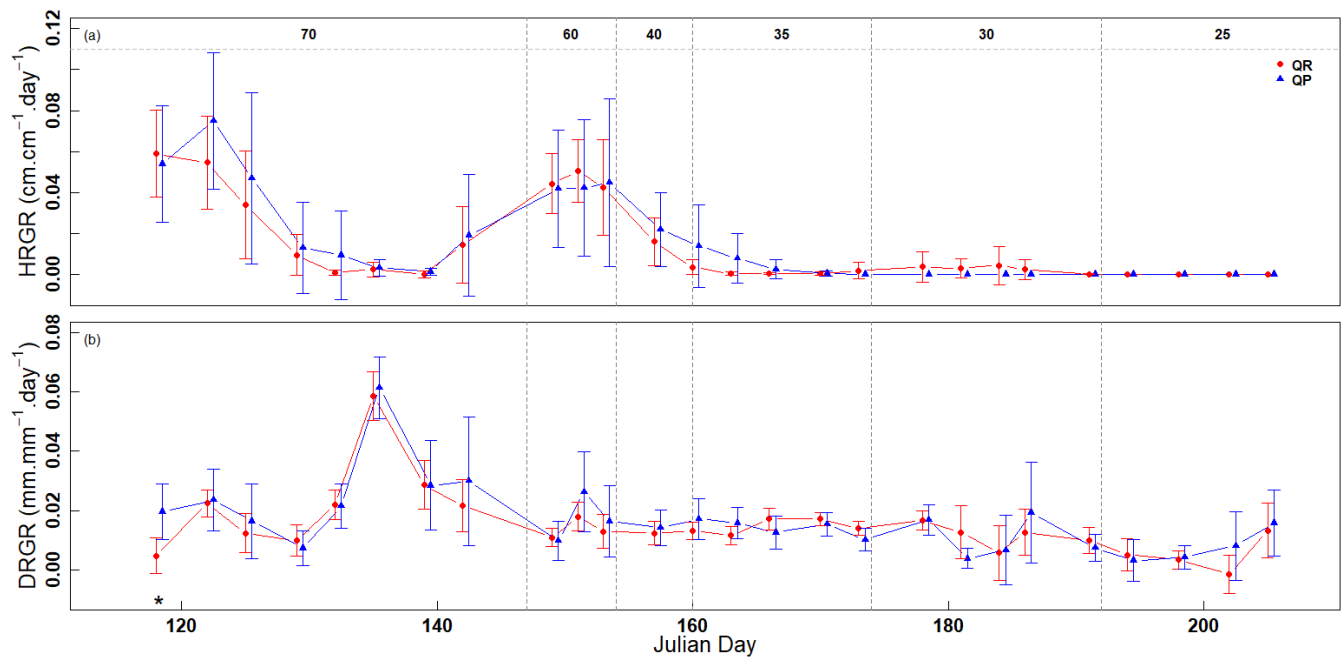
We thank Cyril Buré for the help with growing the seedlings and setting up the experiment on the robotic system. Jimmy for their help in measurements, ONF for harvesting of the seeds.

Annexe

Annexe 1 : Gaz exchange monitoring (An, gs and Wi° results by date. Letters present the results of a Post-hoc Tuckey-HSD test on a two way ANOVA (species and DoY).

%REW		70			60		40	35				30		25	
DoY		143	144	146	152	153	159	165	164	166	173	191	192	200	204
QR	An	bcd	bcd	ab	abc	a	bcd	bcd	bcd	bcd	bc	bc	bcd	bcd	bcd
QP		bcd	bcd	bcd	bcd	ab	bcd	cd	bcd	cd	d	cd	d	cd	cd
QR	gs	abcd	abcde	ab	abc	a	de	de	de	de	cde	de	cde	de	cde
QP		abcd	bcde	abcde	abcde	abcd	abcd	de	de	de	e	de	de	de	de
QR	Wi	d	cd	d	cd	cd	abcd	abc	abcd	abcd	abcd	bcd	abcd	abcd	abcd
QP		d	cd	cd	cd	dc	cd	abcd							

Annexe 2 : The relative height (a) and diameter (b) growth rates (RHGR and DRGR, respectively). With RGR calculated from date to date as $RGR = (\ln X_2 - \ln X_1)/(t_2 - t_1)$ (see Hoffmann and Poorter 2002). With red dots for QR and blue triangles for QP and the %REW changes in vertical dotted line. The differences of growth rates between species at a given date from a t-test are presented as : P values : “****” for $P < 0.001$; “***” for $P < 0.01$ and “*” for $P < 0.05$. To avoid overlapping values and improve the visibility, QP monitoring has been shifted by a day.



Bibliography Article 3 / H2Oak 2017

- Aasamaa K, Aphalo PJ (2016) The acclimation of *Tilia cordata* stomatal opening in response to light, and stomatal anatomy to vegetational shade and its components. *Tree Physiol.* 37: 209-219
- Becker M, Lévy G (1982) Le dépérissement du chêne en forêt de Tronçais. Les causes écologiques. *Ann. Sci. For.*, 39: 439-444.
- Becker M, Lévy G (1986) Croissance radiale comparée de chênes adultes (*Quercus robur* L. et *Q. petraea* [Matt.] Liebl.) sur sol hydromorphe acide. Effet du drainage. *Acta Oecol., Oecol. Plant.* 7 (21): 121-143.
- Bréda N, Cochard H, Dreyer E, Granier A (1993) Field comparison of transpiration, stomatal conductance and vulnerability to cavitation of *Quercus petraea* and *Quercus robur* under water stress. *Ann For Sci* 50:571–582.
- Collet C, Manso R, Barbeito I (2016) Coexistence, association and competitive ability of *Quercus petraea* and *Quercus robur* seedlings in naturally regenerated mixed stands. *For. Ecol. Manage.* 390 : 36–46.
- Damour G, Simonneau T, Cochard H, Urban L (2010) An overview of models of stomatal conductance at the leaf level. *Plant, cell & Environ* 33: 1419–1438.
- Dobrovolný P et al (2016) Recent growth coherence in long-term oak (*Quercus* spp.) ring width chronologies in the Czech Republic. *Clim Res* 70 :133–141.
- Drake PL, Froend RH, Franks PJ (2013) Smaller, faster stomata: scaling of stomatal size, rate of response, and stomatal conductance. *J Exp Bot* 64: 495–505.
- Dumont J, Spicher F, Montpied P, Dizengremel P, Jolivet, Y, Le Thiec, D (2013) Effects of ozone on stomatal responses to environmental parameters (blue light, red light, CO₂ and vapour pressure deficit) in three *Populus deltoides* × *Populus nigra* genotypes. *Environmental Pollution*, 173, 85-96.
- Durand M, Brendel O, Buré C, Le Thiec D (2019) Altered stomatal dynamics induced by changes in irradiance and vapour-pressure deficit under drought : impacts on the whole plant transpiration efficiency of poplar genotypes. *New Phytologist* 222 :1789-1802.
- Epron D, Dreyer E (1993) Long- term effects of drought on photosynthesis of adult oak trees [*Quercus petraea* (Matt.) Liebl. and *Quercus robur* L.] in a natural stand. *New Phytol* 125:381–389.
- Farquhar GD, Caemmerer S Von, Berry JA (1980) A biochemical model of photosynthesis CO₂ fixation in leaves of C₃ species. *Planta* 149: 78–90.
- Fonti P, Heller O, Cherubini P, Rigling A, Arend M (2013) Wood anatomical responses of oak saplings exposed to air warming and soil drought. *Plant Biol* 15:210–219.
- Franks PJ, Farquhar GD (2007) The mechanical diversity of stomata and its significance in gas-exchange control. *Plant Physiol* 143: 78–87.
- Friedrichs DA *et al* (2008) Complex climate controls on 20th century oak growth in Central-West Germany. *Tree Physiol.* 29 : 39–51.

- Gérard B, Alaoui-Sossé B, Badot PM (2009) Flooding effects on starch partitioning during early growth of two oak species. *Trees* 23(2) : 373.
- Gerardin T, Douthe C, Flexas J, Brendel O (2018) Shade and drought growth conditions strongly impact dynamic responses of stomata to variations in irradiance in *Nicotiana tabacum*. *Environ Exp Bot*.
- Gerardin et al., 2019 (unpublished yet)
- Gieger T, Thomas FM (2005) Differential response of two Central-European oak species to single and combined stress factors. *Trees* 19:607–618.
- Granier A, Breda N, Biron P, Villette S (1999) A lumped water balance model to evaluate duration and intensity of drought constraints in forest stands. *Ecological modelling*, 116(2-3) : 269-283.
- Granier A, Ceschia E, Damesin C, Dufrêne E, Epron D, Gross P, Lucot E (2000) The carbon balance of a young beech forest. *Functional ecology*, 14(3) : 312-325.
- Grantz D, Zeiger E (1986) Stomatal responses to light and leaf-air water vapor pressure difference show similar kinetics in sugarcane and soybean. *Plant Physiology* 81, 865-868.
- Haworth M, Marino G, Cosentino SL, Brunetti C, De Carlo A, Avola G, Centritto M (2018) Increased free abscisic acid during drought enhances stomatal sensitivity and modifies stomatal behaviour in fast growing giant reed (*Arundo donax* L.). *Environmental and Experimental Botany*. 147: 116-124.
- Hu B, Simon J, Rennenberg H (2013) Drought and air warming affect the species-specific levels of stress-related foliar metabolites of three oak species on acidic and calcareous soil, *Tree Physiology*, 33 : 489–504.
- Jensen JS (2000) Provenance Variation in Phenotypic Traits in *Quercus robur* and *Quercus petraea* in Danish Provenance Trials. *Scand. J. For. Res.* 15 : 297–308.
- Jones HG (2013) *Plants and microclimate: a quantitative approach to environmental plant physiology*. Cambridge university press.
- Kaiser E, Morales A, Harbinson J (2018) Fluctuating light takes crop photosynthesis on a rollercoaster ride. *Plant physiology*, 176: 977-989.
- Kardiman R, Ræbild A (2017) Relationship between stomatal density, size and speed of opening in Sumatran rainforest species. *Tree physiology*, 38(5), 696-705.
- Kirschbaum MUF, Gross LJ, Pearcy RW (1988) Observed and modelled stomatal responses to dynamic light environments in the shade plant *Alocasia macrorrhiza*. *Plant, Cell Environ* 11: 111–121.
- Kremer A, Petit R (1993) Gene diversity in natural populations of oak species. *Annales des Sciences Forestières* 50 : 186-203.
- Landmann G, Becher M, Delatour C, Dreyer E, Dupouey JC (1993) Oak dieback in France: historical and recent records, possible causes, current investigations. *Rundgespräch der Kommission fuer Oekologie (Germany)*.
- Lawson T, von Caemmerer S, Baroli I (2010) Photosynthesis and Stomatal Behaviour. in 265–304 doi:10.1007/978-3-642-13145-5_11

- Lawson T, Blatt MR (2014) Stomatal size, speed, and responsiveness impact on photosynthesis and water use efficiency. *Plant Physiol* 164: 1556–70.
- Lawson T, Kramer DM, Raines CA (2012) Improving yield by exploiting mechanisms underlying natural variation of photosynthesis. *Curr Opin Biotechnol* 23: 215–220.
- Lévy G, Becker M, Duhamel DA (1992) Comparison of the ecology of pedunculate and sessile oaks: radial growth in the Centre and Northwest of France. *For Ecol Manage* 55:51–63.
- Matthews JS, Vialet-Chabrand SR, Lawson T (2018) Acclimation to fluctuating light impacts the rapidity and diurnal rhythm of stomatal conductance. *Plant physiology*. 176: 1939-1951.
- McAusland L, Vialet-Chabrand S, Davey P, Baker NR, Brendel O, Lawson T (2016) Effects of kinetics of light-induced stomatal responses on photosynthesis and water-use efficiency. *New Phytol* 211: 1209–1220.
- Naumburg E, Ellsworth DS, Katul GG (2001) Modeling dynamic understory photosynthesis of contrasting species in ambient and elevated carbon dioxide. *Oecologia* 126(4) : 487-499.
- Ooba M, Takahashi H (2003) Effect of asymmetric stomatal response on gas-exchange dynamics. *Ecol Modell* 164: 65–82.
- Parent C, Crèvecoeur M, Capelli N, Dat JF (2011) Contrasting growth and adaptive responses of two oak species to flooding stress : role of non- symbiotic haemoglobin. *Plant, cell & environment* 34(7) : 1113-1126.
- PAYAN E (1982) Contribution à l'étude de la croissance rythmique chez de jeunes chênes pedoncules, quercus pedunculata ehrh (Thèse).
- Ponton S, Dupouey JL, Bréda N, Feuillat F, Bodénès C, Dreyer E (2001) Carbon isotope discrimination and wood anatomy variations in mixed stands of *Quercus robur* and *Quercus petraea*. *Plant Cell Environ* 24:861–868.
- Ponton S, Dupouey JL, Bréda N, Dreyer E (2002) Comparison of water-use efficiency of seedlings from two sympatric oak species: genotype x environment interactions. *Tree Physiol* 22:413–422.
- Qu M, Hamdani S, Li W, Wang S, Tang J, Chen Z, Song Q, Li M, Zhao H, Chang T, Chu C, Zhu X (2016) Rapid stomatal response to fluctuating light : an under-explored mechanism to improve drought tolerance in rice. *Funct Plant Biol* 43: 727–738.
- Raven JA (2014) Speedy small stomata? *J Exp Bot* 65: 1415–1424.
- Scuiller I (1990) Exploration de la variabilité des comportements écophysologiques de semis de chênes blancs européens soumis à la sécheresse (Doctoral dissertation, Université Henri Poincaré-Nancy 1).
- Shimazaki K, Doi M, Assmann SM, Kinoshita T (2007) Light regulation of stomatal movement. *Annu Rev Plant Biol* 58: 219–247.
- Team RC (2015) R Foundation for Statistical Computing; Vienna, Austria: 2014. R: A language and environment for statistical computing, 2013.
- Thomas FM (2008) Recent advances in cause-effect research on oak decline in Europe. *CAB Reviews : Perspectives in Agriculture, Veterinary Science, Nutrition and Natural Resources*, 3(037) : 1-12.

- Thomas FM, Gausling T (2000) Morphological and physiological responses of oak seedlings (*Quercus petraea* and *Q. robur*) to moderate drought. *Ann For Sci* 57:325–333.
- Tinoco-Ojanguren C, Pearcy, RW (1992) Dynamic stomatal behavior and its role in carbon gain during lightflecks of a gap phase and an understory Piper species acclimated to high and low light. *Oecologia* 92(2) : 222-228.
- Violet-Chabrand S, Dreyer E, Brendel O (2013) Performance of a new dynamic model for predicting diurnal time courses of stomatal conductance at the leaf level. *Plant, Cell & Environment*. doi: 10.1111/pce.12086.
- Violet- Chabrand SRM, Matthews JSA, McAusland L, Blatt MR, Griffiths H, Lawson T (2017) Temporal dynamics of stomatal behavior : modeling and implications for photosynthesis and water use. *Plant Physiology* 174: 603–613.
- Vico G, Manzoni S, Palmroth S, Katul G (2011) Effects of stomatal delays on the economics of leaf gas exchange under intermittent light regimes. *New Phytol* 192: 640–652 181.
- Vivin P, Aussenac G, Lévy G (1993) Differences in drought resistance among three deciduous oak species grown in large boxes. *Annales des Sciences Forestières* 50 : 221-233.
- Way DA, Pearcy, RW (2012) Sunflecks in trees and forests : from photosynthetic physiology to global change biology. *Tree physiology*, 32(9) : 1066-1081.
- Willaume M, Pagès L (2011) Correlated responses of root growth and sugar concentrations to various defoliation treatments and rhythmic shoot growth in oak tree seedlings (*Quercus pubescens*). *Annals of botany*, 107(4) : 653-662.
- Woods DB, Turner NC (1971) Stomatal response to changing light by four tree species of varying shade tolerance. *New Phytol.* 70: 77–84
- Xiong D, Douthe C, Flexas J (2018) Differential coordination of stomatal conductance, mesophyll conductance and leaf hydraulic conductance in response to changing light across species. *Plant, Cell & Environment* 41: 436–450.